Economic Geology
Vol. 88, 1993, pp. 2154–2181

Metallogenesis in Back-Arc Environments: The Lau Basin Example

YVES FOUQUET,

IFREMER, Centre de Brest, B.P. 70, 29280 Plouzane, France

ULRICH VON STACKELBERG,

Bundesanstalt für Geowissenschaften und Rohstoffe, 3000 Hannover 51, F.R. Germany

JEAN LUC CHARLOU,

IFREMER, Centre de Brest, B.P. 70, 29280 Plouzane, France

JÖRG ERZINGER,

Institut für Geowissenschaften, Justus-Liebig-Universität, 6300 Giessen, F.R. Germany

PETER M. HERZIG,

Institut für Mineralogie und Lagerstättenlehre, R.W.T.H., Aachen, 5100 Aachen, F.R. Germany

RICHARD MÜHE,

Geologisches Institut, Universität Kiel, 2300 Kiel 1, F.R. Germany

AND MICHAEL WIEDICKE

Bundesanstalt für Geowissenschaften und Rohstoffe, 3000 Hannover 51, F.R. Germany

Abstract

Geologic investigations with the submersible *Nautile* in the Lau basin represent one of the first detailed studies of hydrothermal activity on a modern back-arc volcanic ridge, the Valu Fa Ridge. Three major hydrothermal fields (Hine Hina, Vai Lili, and White Church) were discovered in the areas of the greatest differention of volcanic rocks.

The type of hydrothermal deposit is controlled by the type of volcanism and by tectonic activity which increases from south to north. Three stages of sulfide formation are proposed. During the first stage (Hina Hina field), diffuse discharge through volcaniclastic material produces extensive Fe-Mn oxide crusts covering sulfide deposits within the volcanic material. During the second stage (Vai Lili field), tectonic activity increases and fault-controlled discharge forms chimneys on the sea floor. Diffuse discharge is still present. During the third stage (White Church field), hydrothermal activity is completely controlled by major faults and results in the development of sulfide mounds.

Vent fluids at Valu Fa have much higher metal contents than those at midocean ridges. Cl enrichment is best explained by mixing with deep brine rather than by subcritical phase separation and there is no evidence for a magmatic fluid contribution. Some characterictics of the fluids, such as low pH (2) and low concentration of H_2S, can be explained by subsea-floor sulfide formation. The water-rock reaction zone is estimated to be about 1 km below the sea floor and 2 km above the magma chamber.

Vertical mineralogical zonation within the mound differs from midocean ridge deposits but is similar to that of a kuroko deposit. At the surface of the deposit, the virtual absence of pyrite and the high amount of sphalerite, barite, tennantite, galena, and locally, native gold are remarkable. The distinctive chemical characteristics of deposits in each volcanic segment are explained by interaction with variable amounts of differentiated rocks.

Compared to midocean ridges, Lau basin deposits are enriched in Ba, Zn, As, Pb, Ag, Au, and Hg and depleted in Mo, Se, and Co. Relative to young intracontinental back-arc basins (e.g., Okinawa trough), the mineralizations are Pb and As poor. Their mineralogy, chemical composition, and geologic setting show that the southern Lau basin deposits are intermediate between oceanic and continental back-arc deposits.

0361-0128/93/1525/2154-28$4.00

Introduction

DURING recent years, there have been a number of investigations of hydrothermal processes in modern back-arc environments. This tectonic setting corresponds closely to that of ancient major sulfide deposits on land where massive sulfides are commonly associated with felsic volcanic rocks (Franklin et al., 1981; Scott, 1985, 1987; Rona, 1988). These onshore deposits are believed to have formed in island-arc settings or marginal basins (Franklin et al., 1981; Scott, 1985, 1987; Halbach et al., 1989; Sawkins, 1990). The fundamental ore-forming processes in these environments are similar to those described at sea-floor spreading centers; however, the character of the resulting deposits is largely controlled by source-rock lithology reflective of the tectonic setting. Occurrences of hydrothermal deposits in back-arc environments are now known in the Okinawa trough (Halbach et al., 1989, 1993), the Manus basin (Both et al., 1986, Tufar, 1986; Binns and Scott, 1993), the Mariana basin (Craig et al., 1987; Urabe and Kusakabe, 1990), and the north Fiji basin (Auzende et al., 1989; Bendel, 1993; Bendel et al., 1993).

The Lau basin back-arc system can be divided into two major domains: the northern segment, between 17°30′ S and 19°20′ S, located at the central part of the basin, and the southern segment, between 19°20′ S and 22°50′ S (Valu Fa Ridge), located 75 km closer to the arc on the eastern side of the basin (Fig. 1). Detailed investigations to locate the southern back-arc spreading ridges commenced in 1982 (Morton and Sleep, 1985) and the spreading axis, known as the Valu Fa Ridge (Fig. 1), was mapped in detail from 22°50′ S to 20°50′ S between 1984 and 1988 (von Stackelberg et al., 1985, 1988, 1990; Foucher et al., 1988). In 1988, a Gloria side-scan sonar survey gave a general view of the entire spreading system (Parson et al., 1990). Geochemical studies on volcanic rocks show an increasing influence of the arc components from north to south (Hawkins and Melchior, 1985; Jenner et al., 1987; Volpe et al., 1988; Boespflug, 1990; Frenzel et al., 1990; Loock et al., 1990; Sunkel, 1990).

The first indication of a hydrothermal deposit, consisting of silica and barite, was reported on the Peggy Ridge by Bertine and Keene (1975; Fig. 1a). Sulfides are also known in the northern part of Lau basin (Hawkins and Helu, 1986). The indications of hydrothermal activity along the Valu Fa Ridge were obtained between 1984 and 1990 (von Stackelberg et al., 1985, 1988, 1990a and b; Herzig et al., 1990; von Stackelberg and von Rad, 1990) and in 1989,

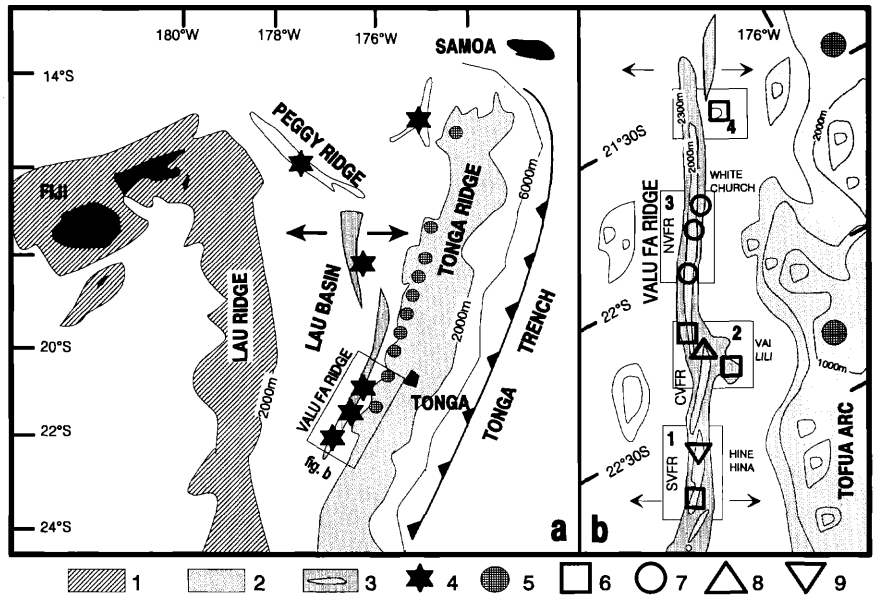

FIG. 1. a. General map of the Lau back-arc basin. b. Location of the hydrothermal fields along the Valu Fa Ridge near the active Tofua island arc. The four diving areas (1, 2, 3, 4) are shown together with the names of the three main hydrothermal fields (Hine Hina, Vai Lili, and White Church). Nine hydrothermal occurrences were found along the Valu Fa Ridge. 1 = Lau Ridge, a remnant island arc; 2 = Tonga Ridge, an island arc; 3 = active back-arc spreading—light dots are above 2,000 m; 4 = hydrothermal occurrences in the Lau basin; 5 = active volcanoes, the active part of the island arc (Tofua arc); 6 = Fe-Mn deposits; 7 = Ba-Zn deposits; 8 = Zn-Ba-Cu-Fe deposits; 9 = Fe-Cu sulfides under Fe-Mn crusts.

during submersible investigations, widespread and intense hydrothermal activity was discovered here (Fouquet et al., 1990, 1991a, b). Recently, a diving program with the Russian *Mir* submersible in the northern Lau basin found extensive inactive sulfides deposits associated with andesitic lava at 15°23′ S, and with basalt at 18°36′ S (Malahoff and Falloon, 1991; Fig. 1a).

In this paper we present results obtained in 1989 during the 24-day French-German diving cruise Nautilau. Data on the tectonic setting, mineralogy, and geochemistry of the newly discovered deposits and associated hydrothermal waters are used to interpret the metallogenic processes in a back-arc environment. In addition, data on the geochemistry of the volcanic rocks associated with the deposits are discussed. A comparison is made between hydrothermal deposits observed at nine different places along a distance of more than 120 km (Fig. 1b). Finally, similarities and differences between the Lau basin, midocean ridge, other back-arc, kuroko-type, and Archean volcanogenic sulfide deposits are discussed.

Geologic Setting: The Lau Basin

The Lau basin is a typical example of an active back-arc basin between a remnant arc (Lau Ridge) and an active volcanic arc (Tofua volcanic arc) behind the westward-dipping Tonga-Kermadec subduction zone (Fig. 1 a and b). Lau basin was once considered to be one of the simplest of the world's back-arc basins formed by arc splitting (Karig, 1971). It has a triangular shape with a width of 600 km in the north and only 200 km in the south, suggesting that the basin is opening by propagation toward the south. The northern spreading axis at the center of the basin, composed of tholeiitic basalt with midocean ridge basalt (MORB) composition, started to open 3 to 5 m.y. ago (Cherkis, 1980; Malahoff et al., 1982). Recent Ocean Drilling Program drilling has revealed that, following a period of basin-and-range-type extension, organized sea-floor spreading started only 1 to 2 m.y. ago (Ocean Drilling Program Leg 135 Scientific Party, 1992).

The Valu Fa Ridge is the active back-arc spreading center of the southern Lau basin between 21° and 23° S (Morton and Sleep, 1985; von Stackelberg et al., 1985, 1988; Foucher et al., 1988; Morton and Pohl, 1990; Parson et al., 1990). Opening started 1 m.y. ago with 3 cm/yr half-spreading rate. The Valu Fa Ridge, located only 20 to 40 km west of the active Tofua volcanic arc (Fig. 1), is more than 150 km long and generally strikes 20° (NNE); it is 2 to 5 km wide and rises 500 to 600 m above the surrounding sea floor. Small nontransform offsets and an overlapping spreading center divide the ridge into three major segments: the southern, central, and northern Valu Fa Ridge (von Stackelberg et al., 1988, von Stackelberg and von Rad, 1990) which are arranged en echelon a few kilometers apart. The southern Valu Fa Ridge is still propagating southward. The individual volcanic segments consist of small, straight ridges, predominantly with steep slopes. South of 22°45′ S, the southern Valu Fa Ridge gradually disappears. The crestal area is commonly only a few hundred meters wide and covered with volcaniclastic debris. During the Nautilau dives, a transversal asymmetry of the ridge and the absence of an axial graben structure were noted indicating a complex tectonic system compatible with a strike-slip component proposed in geodynamic models (Pelletier and Louat, 1989). The high gas content of the magma has produced very vesicular and brecciated lavas, whereas major faults and fissures are less numerous than at midoceanic ridges. At central Valu Fa Ridge, a 1- to 2.5-km-wide magma chamber has been imaged seismically under the neovolcanic zone at a depth of about 3 km below the sea floor (Morton and Sleep, 1985; Collier and Sinha, 1990). The magma chamber was imaged beneath an entire 35-km-long segment including the overlapping spreading center and the Vai Lili active hydrothermal field.

Morphology and Tectonic Fabric of the Valu Fa Ridge

Southern Valu Fa Ridge

The ridge is approximately 20 km long and displays four bathymetric highs; the two southernmost highs, which were targets for our diving campaign, are the shallowest, rising up to a 1,820-m water depth. Only a few fault scarps were seen in the crestal area, at one location with nearly vertical walls up to 15 m high. The most remarkable observation was the smooth surface of vast areas at the ridge crest. However, it seems that a volcaniclastic cover is effectively masking some of the tectonic features. Recent tectonic extension can be deduced from the presence of small predominantly ridge-parallel cracks, both open and sealed, and observation of sealed and open small cracks within hydrothermal crusts covering the sea floor (von Stackelberg and Wiedicke, 1990). The extended low-temperature Hine Hina field is located within this area.

Central Valu Fa Ridge

This segment is about 30 km long and composed of three subsections. Diving concentrated on the shallow northern section (min water depth = 1,600 m) which forms a 9-km-long overlapping spreading center with the northern Valu Fa Ridge. Here, the central Valu Fa Ridge is particularly steep and narrow with a triangular cross sectional shape typical for ridge axes near discontinuities (Macdonald et al., 1988). Volcanic mounds up to 60 m high were encountered along the crest of the central Valu Fa

Ridge. The structural grain at the upper flanks and the crest, as observed by side-scan sonar, is dominantly linear and ridge-parallel. A microrelief of 0.5 to 3 m caused by closely spaced fissures, small faults, and grabens indicates tectonic extension (Wiedicke and Kudrass, 1990). This fabric is particularly well developed in the northernmost section, where the high-temperature Vai Lili site is located. A number of ridge-parallel normal faults with a 5- to 10-m throw were observed at the upper western and eastern flanks.

Northern Valu Fa Ridge

Except for its southern end, this ridge segment is slightly deeper (1,850–1,970 m) than the central Valu Fa Ridge. The area is affected by intensive medium-scale faulting with numerous fault scarps of 5 to 1 5 m throw (max 60 m). The fault scarps are commonly inward facing but some long, talus-rich sections with particularly steep slopes represent outward-facing normal faults. The inactive hydrothermal White Church site is located close to a saddle point of this ridge segment and related to a major fault. Compared with the central Valu Fa Ridge, the intensive medium-scale faulting at the northern Valu Fa Ridge indicates an advanced stage of destruction in the volcano-tectonic cycle controlling crustal accretion at the Valu Fa Ridge (Wiedicke and Kudrass, 1990).

Setting and Description of Major Hydrothermal Sites

Southern Valu Fa Ridge (Hine Hina field)

The bathymetric high of the southern Valu Fa Ridge is an area of widespread low-temperature hydrothermal activity. Numerous locations where clear fluid is discharging diffusely at 40°C are commonly densely populated with vent fauna, e.g., mussels, shrimps, white crabs, fish, etc. The observed discharge is restricted in general to the crestal area above the 1,900-m isobath (Fig. 2). The sea floor in the immediate vicinity of these sites is white and resembles a snow field or a glacier. It is composed of strongly bleached, altered, and distintegrated volcanics displaying a characteristic white color ("Hine Hina" is Tongan for "white"; Fig. 3e and f). The altered volcanics show veinlike and disseminated sulfide mineralization.

The dominant rock types exposed in this area, particularly at the upper ridge flanks, are brecciated lava and dark volcaniclastic sands. Vast areas between the white-colored sites are covered with black Mn crusts (Fig. 3g) associated with shells of dead mussels. The extension along the ridge axis is at least 2 km (Fig. 2). The Mn oxides cover angular rock outcrops and impregnate and indurate volcaniclastic sands, preserving fossil ripple marks in the sand. At the ridge flanks and in distal parts of this site, black flow lines of transported Mn oxides were seen. Dark and light mottling of the sands indicates subsurface Mn-Fe-rich layering exposed at the sea floor by bioturbation. Black Mn precipitates form small 20-cm-high caulifower-shaped mounds (Fig. 3h). Sampling indicates that the crusts in general are several centimeters thick. They are commonly laminated and expose an ocher-colored Fe-rich lower layer. In places several generations of such black and ochre crusts have precipitated at the sea floor. Shimmering water (about 10°C) was pouring out from cracks and from holes a few centi-

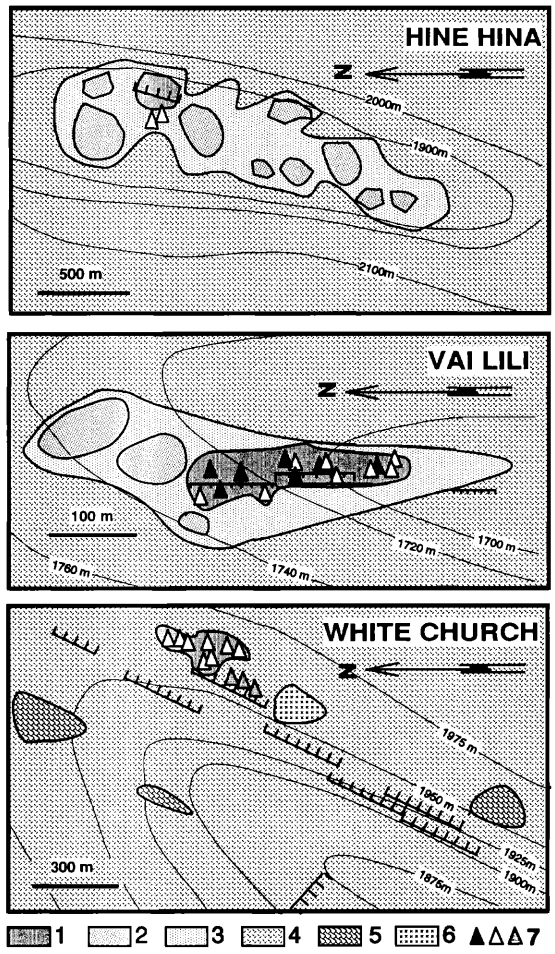

FIG. 2. Schematic geologic map of the three main hydrothermal fields. See location in Figure 1b. 1 = sulfide deposit; 2 = area of active diffuse low-temperature (< 40°C) discharge; 3 = Mn crust and/or Fe impregnation within volcaniclastics; 4 = dominant volcaniclastic rocks; 5 = pillow lava; 6 = field of pumice; 7 = hydrothermal chimneys. Black = active black smokers (Vai Lili); white = active white smokers (Vai Lili field) and Ba-dominant inactive chimneys for the other fields; gray = Mn chimneys along faults; heavy dark lines = normal faults; ticks are on downthrown side of faults.

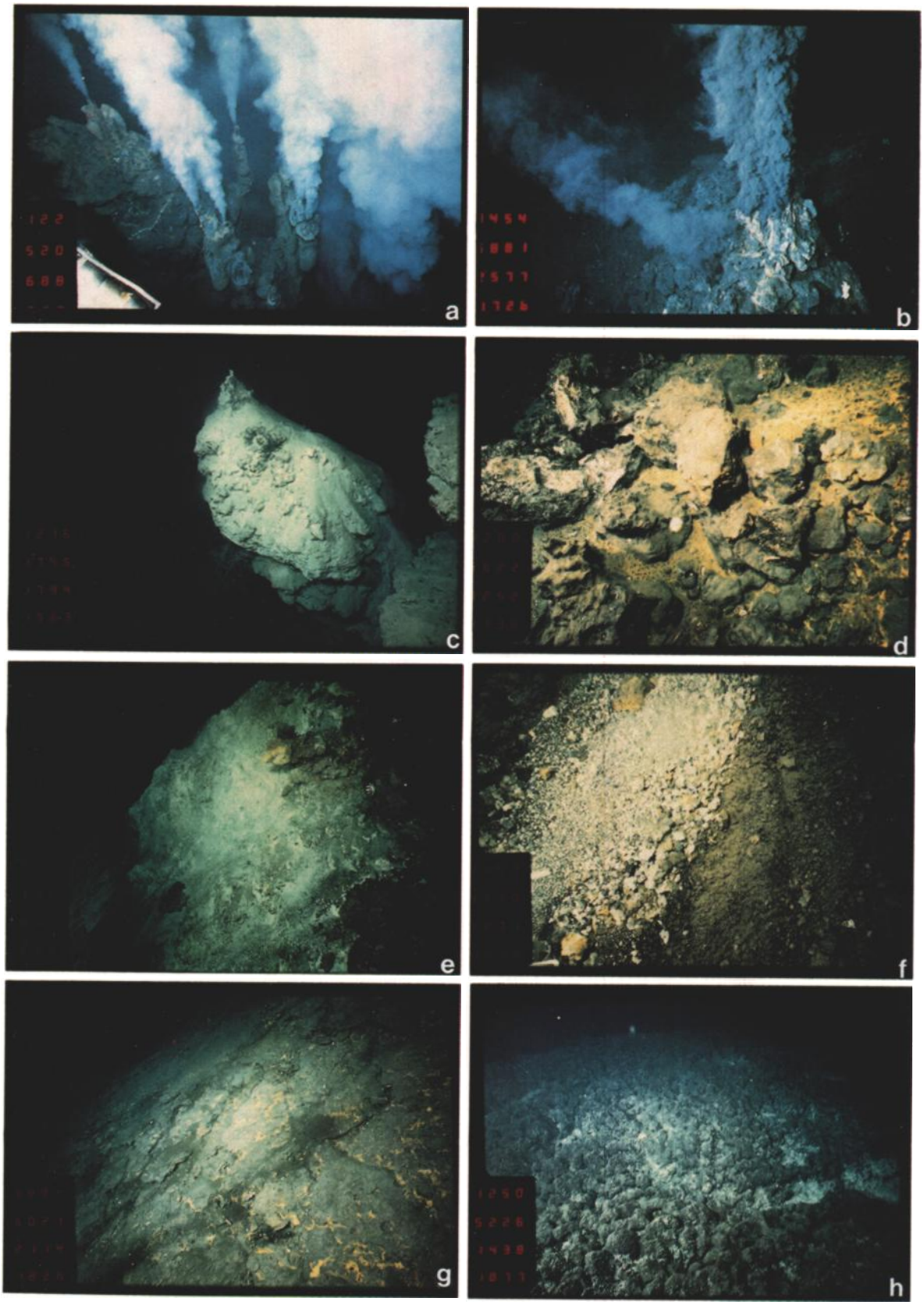
a
b
c
d
e
f
g
h

meters in diameter. Cracks within the crusts are commonly healed by protruding seams of Mn precipitate.

On the upper eastern slope an extensive outcrop of white altered volcanic sands with disseminated pyrite crystals was observed and sampled (Fig. 4b). The bleached clastic material is covered by a layer of volcaniclastics cemented by massive copper-rich sulfides. The outcrop is capped by an Mn crust pierced by 13 brown inactive nodular chimneys up to 2 m high, composed of barite and sphalerite. Since the crusts and chimneys are slightly inclined toward the west, recent tilting of a crustal block has led to the formation of this outcrop. A dive (Fig. 2) along an elevation in the southern prolongation of the Hine Hina area found low-temperature hydrothermal deposits such as Fe and Mn crusts covering brecciated lava and volcaniclastic sediments. In the same area, faulted massive lava was observed on the western flank of the volcanic ridge 60 to 120 m deeper than the ridge crest. Temperature anomalies up to 0.05°C indicate that these faults are preferential pathways for discharging fluids and that there is a more massive nonbrecciated, but still highly vesicular, lava beneath the volcaniclastic material.

Central Valu Fa Ridge (Vai Lili field)

A vigorously active site (Fig. 3a) with numerous discharging fluids up to 342°C lies at the upper western flank of the central Valu Fa Ridge within the portion that overlaps with the northern Valu Fa Ridge. Low-temperature hydrothermal activity indicated by shimmering water (15°C) and Mn-Fe precipitates was observed at the southernmost part of the northern Valu Fa Ridge overlapping with the central Valu Fa Ridge. At the central Valu Fa Ridge the hydrothermal deposits are mainly found along faults disrupting the prevailing sheet lavas. The site is about 400 m long and 100 m wide. It is directly related to north-south-trending normal faults with up to 15 m vertical offset in a water depth of 1,720 m (Figs. 2 and 4a). Black smokers (Fig. 3b) were observed in the immediate vicinity of the fault, whereas white smokers were located nearby (Fig. 3a), both at the base and at the top of the fault. Between the different groups of chimneys, sulfides form an irregular mound (Fig. 3d) 200 m long and 50 m wide. Mn precipitates are related to diffuse warm water discharge between the chimneys. In addition, Mn and Fe oxides, related to extensive active diffuse discharge, form a continuous halo around this deposit and extend the hydrothermal activity of the site toward the north and south along the crest of the central Valu Fa Ridge (Fig. 2). Black and white smokers built different chimneys: the black smokers are about 2 to 5 m high and commonly feature numerous outlets (that look like organ pipes), whereas white smokers form treelike stems

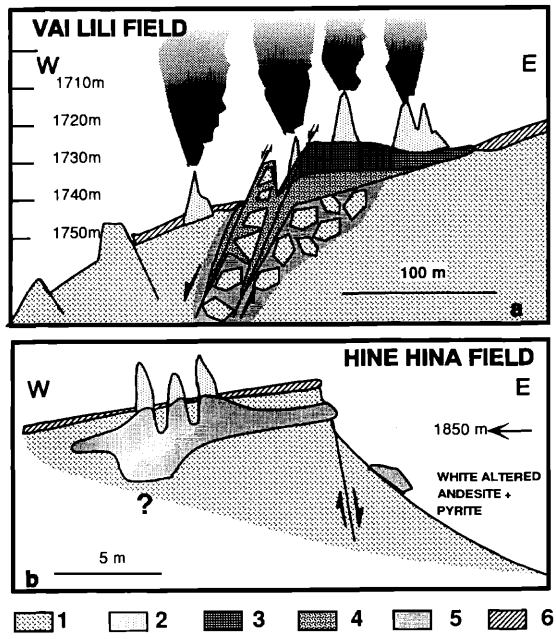

FIG. 4. a. Vertical section across the Vai Lili deposit at 22°13′S on the western flank of the central Valu Fa Ridge. Active smokers were seen both at the base and at the top of a normal fault. Black smokers were close to, or directly on, the fault. White smokers were on both sides. The thickness of the Mn crust is exaggerated. b. Schematic cross section of an outcrop of a pyroclastic layer at the southern end of the Hine Hina field, southern Valu Fa Ridge (see Figs. 1 and 2). The layer is cemented by marcasite, pyrite, and chalcopyrite with minor barite. It is covered by an Mn-Fe crust and underlain by strongly altered and disintegrated white volcanic material with pyrite. Ba-Zn chimneys, probably connected to the massive sulfide horizon underneath, are growing at the top. The crust played the role of sealing the rocks and enhancing the effects of hydrothermal alteration and sulfide deposition. 1 = brecciated andesites, 2 = Ba-Zn chimneys, 3 = Zn-Ba massive mound, 4 = Cu-Fe massive core, 5 = stockwork, 6 = Mn-Fe crust on volcaniclastic material.

FIG. 3. Photos obtained with the 24-mm camera installed on the *Nautile*, the field of view is between 7 and 10 m wide. a. White smoker group (Vai Lili field). Water depth is 1,720 m. b. Black smoker (Vai Lili field). Water depth is 1,720 m. c. White inactive barite-sphalerite chimney (White Church field). d. Talus of Cu-rich massive sulfides at the foot of a normal fault (Vai Lili field). e. Highly altered andesite (white) and Cu-Fe massive sulfides blocks (brown) from a massive sulfide layer formed within the andesite (Hine Hina field). f. Highly altered volcaniclastic andesite at the upper part of the volcanic ridge (Hine Hina field). g. Mn crust occurring as plates. Along the small cracks the yellow color indicates an increase of Fe under the Mn crust (Hine Hina field). h. Mn crust occuring as cauliflowerlike structures (Hine Hina field).

up to 15 m high and 1 to 2 m thick; the latter show a decimetric to centimetric horizontal layering with thick horizontal protrusions resembling cactus leaves with white, yellow, and red coverings.

At the scarp of the north-south-trending fault, a complete cross section through the massive sulfide deposit has been exposed (Fouquet et al., 1991b; Fig. 4a). From the top to the base are observed (1) a vigorously active black smoker (342°C; 1,727-m water depth), (2) talus of immature sulfides produced by broken chimney fragments (1,731 m), (3) boulders of massive Cu-rich sulfides representing the core of the deposit exposed along the fault (1,735 m; Fig. 3d), and (4) centimeter-thick veins of Cu- and Zn-rich sulfides in altered volcanics representing a stockwork mineralization (1,739 m). To the south, the stockwork was observed at a 1,727-m water depth near another black smoker at 1,723 m. Ongoing tectonic activity seems in part responsible for the numerous broken chimneys, thus limiting their size. The dominant rock type around this site is brecciated lava, forming eruptional cones aligned along the ridge crest. The relief is >30 m with the depressions and the ridge slope often covered with black rippled glass sand and volcaniclastic debris. Faunal activity at this site is minor in comparison with hydrothermal areas at midocean ridges. Animals only occasionally were seen clustered around white chimneys (small shrimps, large gastropods, and white crabs).

Northern Valu Fa Ridge (White Church field)

A large inactive site was found at the upper eastern flank of the northern Valu Fa Ridge at water depths between 1,966 and 1,946 m (Fig. 2). The field extends over 300 m following the foot of a ridge-parallel, 60-m-high, outward-facing, normal fault. Over an area about 200 m in diameter, numerous, commonly white, chimneys (White Church site; Fig. 3c) composed of barite with disseminated sulfides were encountered. Many of the chimneys are 10 to 15 m high and about 2 to 3 m in diameter, and their shape is characterized by horizontal layers. South of this site a great number of small Mn chimneys (10–50 cm high) occur on talus at the foot of a fault scarp over a distance of more than 100 m.

The lithology of this ridge segment is characterized by frequent changes between dominantly brecciated lava locally alternating with pillow and sheet lavas. A pumice field is located in the immediate neighborhood of the hydrothermal site at the foot of the faults (Fig. 2), and nearby, there is a relatively fresh untectonized pillow field. In contrast, the volcanics at the crest of the ridge are older and covered with a thin veneer of sediment (see also von Stackelberg and Wiedicke, 1990).

About 4 km south of the White Church site (Fig. 1) a 3-m-high inactive Mn-encrusted sulfide chimney was sampled at the crest of the northern Valu Fa Ridge. Hydrothermal sediment, broken chimneys, and large sulfide slabs cover an area 30 × 20 m at water depths of 1,822 to 1,841 m along a talus-covered fault scarp subparallel to the ridge.

About 10 km south of the White Church site, the northern Valu Fa Ridge displays an asymmetric cross section with a gentle western and a steep eastern slope. The dominant rock type is brecciated lava with some pillow lavas. At the crest, a collapsed sulfide-barite chimney was observed in the vicinity of a small 20- × 10-m area of abundant animal life. Within this brecciated lava field, there is a small lava mound with several fluid outlets discharging fluids at 25°C. Mn crusts and several patches of whitish precipitates also occur.

Geochemistry of Volcanic Rocks

In the northern Lau basin, Hawkins and Melchior (1985) have shown an east-west magmatic zonation related to the early stage of opening and the present-day spreading. The composition of the volcanic rocks varies from basalt enriched in lithophile elements, rare earth elements, and volatiles to a normal MORB. In the southern basin, along the Valu Fa Ridge, the situation seems to be similar. At the early stage of opening, magma was depleted in Ni, Co, and Cr and enriched in the lithophile elements Sr, Rb, and Ba compared to MORB. These rocks are, in part, highly differentiated and comprise basalts to dacites (Hawkins and Melchior, 1985; Jenner et al., 1987; Volpe et al., 1988; Beck, 1990; Boespflug et al., 1990; Frenzel et al., 1990; Loock et al., 1990; Sunkel, 1990). Low potassium and high aluminum contents indicate a clear affinity with low potassium arc andesites. Trace element and isotope studies show evidence of an increasing influence of components derived from the subduction slab on the composition of the lavas from north to south (Jenner et al., 1987; Volpe et al., 1988; Beck, 1990; Boespflug et al., 1990; Frenzel et al., 1990; Loock et al., 1990; Sunkel, 1990).

During the Nautilau cruise, as during the Sonne cruises (legs 35, 48, and 67), rock samples were recovered along the Valu Fa Ridge from 21°50′ N (NVFR) to 22°45′ S (SVFR). The average composition of about 100 samples of volcanics that were analyzed from the three areas under investigation are presented in Table 1 and compared with normal MORB. The average distance between the sample locations is about 1.2 km, which allows geochemical mapping of the Valu Fa Ridge on a very fine scale. Figure 5 shows the different rock types along the Valu Fa Ridge ranging from basalt to dacite. The north-south plot displays three distinct areas with more highly differentiated rocks, around 21°55′ S, 22°13′ S, and 22°33′ S. These locations are related

TABLE 1. Average Compositions of Volcanic Rocks

	NVFR	CVFR	SVFR	MORB
Number of samples	25	42	32	
SiO_2 (wt %)	54.84	57.10	56.05	50.45
TiO_2	01.08	01.39	01.35	01.62
Al_2O_3	15.41	15.03	15.05	15.26
FeO_{total}	09.89	10.21	10.53	10.43
MnO	00.18	00.21	00.19	00.18
MgO	04.96	03.26	03.81	07.58
CaO	09.38	07.55	08.00	11.30
Na_2O	02.73	03.40	03.07	02.68
K_2O	00.35	00.47	00.54	00.11
P_2O_5	00.15	00.23	00.19	00.15
H_2O^+	01.06	01.29	01.14	00.30
Total	100.03	100.14	99.92	100.06
Ba (ppm)	80	96	113	14
Cu (ppm)	63	59	57	74
Zn (ppm)	90	100	92	78
Pb (ppm)	1.10	1.30	1.20	0.49

NVFR = northern Valu Fa Ridge, CVFR = central Valu Fa Ridge, SVFR = southern Valu Fa Ridge, MORB = midocean ridge basalt

Pb data are calculated for the less differentiated rocks (basalts and basaltic andesites; $n = 29$); major elements were determined by X-ray fluorescence (R. Mühe, unpub. data); data from Sunkel (1990) are included; trace elements were analyzed either by XRF ($n = 64$) or by ICP-MS ($n = 35$); Pb was analyzed by ICP-MS (D. Garbeschönberg, Univ. of Kiel, FRG, analyst); MORB data are from Hoffman (1988) and Wilson (1989)

geographically to the largest hydrothermal fields (Fig. 5).

In Figure 6, Zn, Ba, Cu, and Pb data have been plotted against SiO_2 separately for each area. Average rocks from the central Valu Fa Ridge have the highest Zn and Pb but lower Cu and Ba values. Volcanics from northern Valu Fa Ridge have highest Cu but lowest Zn, Ba, and Pb contents. Contrary to the results of other authors, cited above, detailed analysis based on Ce/Pb ratios (Mühe, 1991) indicates that the influence of the arc and the subducting slab on the composition of the volcanics is stronger at northern Valu Fa Ridge than at central Valu Fa Ridge and southern Valu Fa Ridge. Thus, even if the active ridge is propagating south, the arc influence is variable and does not show a continuous southward effect. This is perhaps related to the fact that the White Church area is closer (20 km) to the volcanoes of the active Tofua arc than are the Vai Lili (42 km) and Hine Hina fields (43 km; Fig. 1b).

Water Chemistry

In the Vai Lili area several groups of black and white smokers were discovered. Hot fluids were collected on white smokers with maximum exit temperatures of 334°C at vent VL-3, 285°C at VL-2, and 280°C at VL-1. VL-1 was collected at the base of a normal fault; the two other sampling locations are at the top of the same fault. All temperature measurements were carried out repeatedly using the submersible temperature probe; they proved to be internally consistent with a reproducibility of better than ±2°C. A calibration of the probe showed a accuracy of better than ±1 percent up to 400°C. The range of exit temperatures was also determined in other areas. Temperature anomalies in ambient seawater on the sea floor in the vicinity of the vents can reach up to 30°C. This is due to intense diffuse fluid discharge through the highly porous andesite around the chimneys. Hydrothermal plumes with seawater enriched in silica, methane, and Mn and depleted in dissolved oxygen rise up to 200 m above the sea floor.

Samples were collected in modified titanium syringes described by von Damm et al. (1985a). Shortly after recovery by the *Nautile*, the fluids were degassed using a special apparatus. Methane was determined immediatly on board ship and the residual gases were collected in glass and copper tubes for further analyses on shore. Determinations of pH, sulfate, and dissolved silica were completed within a few hours for the VL-2 and VL-3 samples. All fluids were acidified with suprapure HNO_3 and, without being filtered, stored in Nalgene bottles. The samples were then analyzed on shore using titration, photometry, AAS, ICP-AES, ICP-MS, and ion chromatography. The gases were analyzed using a mass spectrometer. During sampling only some ambient seawater was drawn in, and with one exception, all syringes contained >90 percent hydrothermal fluids. The fluid composition was calculated for an Mg-free end member (von Damm et al., 1985a and b). An example is shown for Mn in Figure 7. Samples collected at the upper part of the fault are on the same line whereas

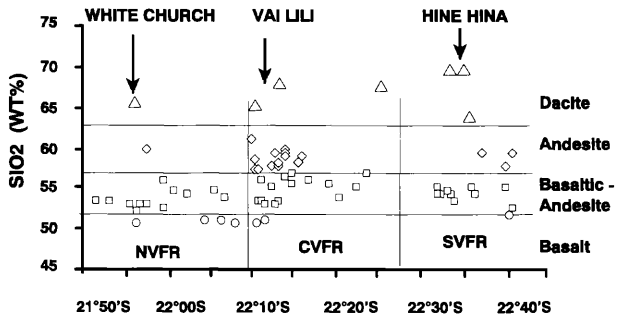

FIG. 5. Silica contents of volcanic rocks along the Valu Fa Ridge. Data are from SO-67, SO-35, and the Nautilau diving campaign. These data are plotted along a north-south transect of the three segments. Horizontal lines define fields of basalts, basaltic-andesites, andesites, and dacites. The approximate location of the three main hydrothermal areas (White Church, Vai Lili, and Hine Hina) are indicated by arrows. The vertical lines represent the structural limit between the northern (NVFR), central (CVFR), and southern (SVFR) Valu Fa Ridges.

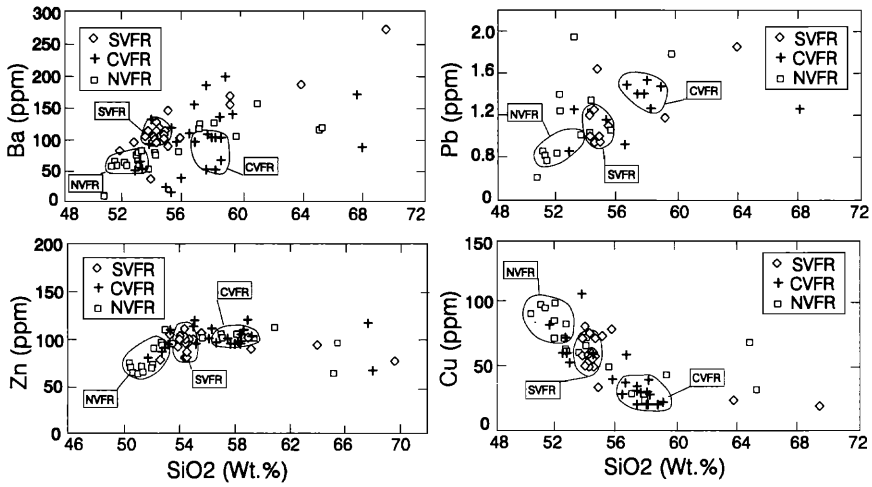

FIG. 6. Plots of Ba, Zn, Pb, and Cu vs. SiO_2. Data for each ridge segment have been plotted separately. In addition, after excluding the evolved rocks that are comparatively less common, areas of highest data concentration for each segment have been drawn. The areas do not overlap and therefore can be used to estimate the available amount of each element in each segment that could be leached from the host rocks by hydrothermal water-rock interactions and serve to form hydrothermal precipitates. The northern Valu Fa Ridge has highest amount of Cu but the lowest Zn, Ba, and Pb; the southern Valu Fa Ridge has the highest amount of Ba but median amounts of Cu, Zn, and Pb.

samples collected at the base are on a different line. The fluid chemistry data are presented in Table 2.

In Figure 8 pathways for fluid ascending with a high flow rate are shown for adiabatic discharge and discharge with additional conductive cooling. The fluid chemistry is mainly controlled by seawater-rock interaction at greenschist facies conditions. The most surprising feature of the samples is the very low pH value of 2, the lowest ever measured in sea-floor hydrothermal fluids. Concentrations of several elements in the Vai Lili fluid differ significantly from fluids debouching at midocean ridges. Contents of K, Rb, Ce, B, and Ba are the highest observed in any sediment-starved sea-floor hydrothermal system. These elements are usually more highly concentrated in andesitic rocks than in midocean ridge basalts. During storage of the samples, small quantities of barite with measurable Sr contents precipitated from the fluids. Thus the reported Ba and Sr concentrations (Table 2) are minimum values. Calcium and Sr correlate positively with chloride which is also the case for midocean ridge fluids (Palmer and Edmond, 1989a and b). These authors concluded that chloro complexing controls the chemical behavior of Ca and Sr in hydrothermal fluids. The $^{87}Sr/^{86}Sr$ values are almost identical for all vents and are slightly higher than for fresh basement rocks from the Valu Fa Ridge ($^{87}Sr/^{86}Sr$ = 0.7033–0.704; Loock et al., 1990). This can be interpreted by fixation of about 85 percent of the seawater Sr in the oceanic crust in the down-welling limb of a hydrothermal circulation cell (Fig. 8). Thus, most of the Sr in the vent fluids was leached out of the basement in the main reaction zone. Using the method of Piepgras and Wasserburg (1985) based on strontium isotopes, the calculated water/rock ratios for the Vai Lili white smokers is about 2.7. This is a maximum, which might be smaller if equilibrium of the reaction was not reached. Water/rock ratios can also be calculated assuming that a particular element is leached quantitatively from the rocks into solution and that the fluid values are corrected for original seawater concentrations. Elements like K, Rb, Li, and B are believed to be almost completely soluble under these conditions and their concentrations in the fluids are not controlled by mineral phase equilibrium reactions. The calculated water/rock ratios between 1.5 and 2 for all vents and all elements mentioned is similar to those found for other hydrothermal systems (Michard et al., 1984; Bowers et al.,

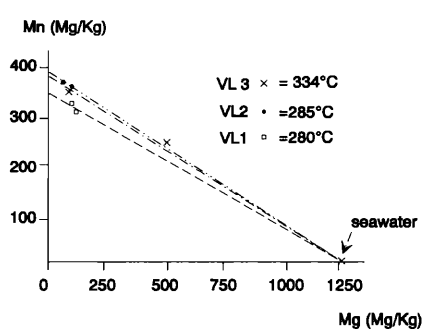

FIG. 7. Manganese end-member concentrations of vent fluids calculated by extrapolation from seawater to Mg = 0 mg/kg.

TABLE 2. Compositions of Vai Lili End-Member Hydrothermal Fluids

	VL-1	VL-2	VL-3	MOR fluids[1]	Seawater
Temperature (°C)	280	285	334	200–350	2
pH (25°C)		2	2	3.2–3.9	7.8
SiO_2 (mM)		13.8	14.5	15.6–23.3	0.15
Li (μM)	580	652	623	843–1,810	25
Na (mM)	552	615	590	432–800	468
K (mM)	64	75	79	23.2–51.6	10.2
Rb (μM)	59	67	68	10–37	1.4
Cs (nM)	1,060	1,370	1,560	177–368	2.2
Cl (mM)	712	804	790	489–1,090	546
Br (μM)	983	1,180	1,140	802–1,832	840
Br/Cl (10^{-3})	1.38	1.47	1.44	1.52–1.70	1.54
SO_4^{-2} (mM)	0	0	0	0	28.2
Mg (mM)	0	0	0	0	53.2
Ca (mM)	35.5	41.3	41.3	9.9–96.4	10.3
Sr (μM)	106	126	20	50–312	90
$^{87}Sr/^{86}Sr$	0.7044	0.7044	0.7044	0.7028–0.7036	0.7091
Ba (μM)	>60	>20	>39	>16	0.14
Fe (mM)	1.16	1.47	2.5	0.75–18.7	1×10^{-6}
Mn (mM)	6.2	7	7.1	0.49–4.48	1×10^{-7}
Fe/Mn	0.19	0.21	0.35	0.9–5.2	
Cu (μM)	16	22	34	2–44	0.004
Zn (mM)	1.4	2.8	3	0.005–0.9	1×10^{-6}
Cd (μM)	0.7	1.4	1.5	0.02–0.18	0.001
Pb (μM)	7	3.8	3.9	0.18–0.36	1×10^{-5}
As (μM)	11	8	6	0.2–0.5	0.023
B (mM)	0.77	0.87	0.83	0.50–0.55	0.416
$\delta^{11}B$ (‰)[2]	25.5	26	26	26.5–33.0	40

Vai-Lili data are mean values of two samples, with end-member concentrations calculated by linear extrapolation to Mg = 0 mM; mM = mmole/kg, μM = μmole/kg, nM = nmole/kg

[1] Data showing the composition range of MOR fluids come from the following references: EPR (East Pacific Rise) = Von Damm et al. (1985); MARK (Mid-Atlantic Ridge-Kane fault zone) = Campbell et al. (1988); SJFR (southern Juan de Fuca Ridge) = Von Damm and Bischoff (1987); seawater = Bruland (1983); other data = Campbell and Edmond (1989), Palmer and Edmond (1989)

[2] Relative to NBS SRM 951

1985, 1988; von Damm et al., 1985a, 1988; Campbell et al., 1988a, b).

Fe and Cu correlate positively with the exit temperatures, and it seems that Zn and Cd behave in the same way. Pb and As also depend on fluid temperature but are inversely related. Concentrations of these chalcophile elements are assumed to be controlled by sulfide solubility and Cu and Fe precipitation in the stockwork zone. Again, concentrations in the vent fluids of Zn, Pb, As, Cd, as well as Mn, are the highest ever measured at the ocean floor. Cu and Zn values cannot be explained by higher contents of these elements in andesites compared to MORB (Table 1). However, concentrations of the chalcophile elements in the rocks depend on the degree of differentiation (Fig. 6).

The quartz saturation in water decreases with decreasing pressure, thus the silica content of the fluid can be used to estimate the depth of the reaction zone. The dissolved silica concentrations at Vai Lili are lower than in most midocean ridge vent fluids, probably due to a shallower depth of both the ocean floor (1,700 m) and the main reaction zone in the crust. With the help of the quartz barometer and using the quartz solubility curves of Bowers et al. (1988), the depth of the main reaction zone is estimated to be about 1 km below the sea floor.

The chondrite-normalized rare earth element patterns of Vai Lili fluids (Fig. 9) are similar to patterns reported for midocean ridge fluids (Michard, 1989). However, REE concentrations are about one order of magnitude higher in Vai Lili fluids and the enrichment in light REE is not so large. La and Lu concentrations in these fluids are up to 1,000 times that of seawater. Low pH, high temperature, and low oxygen fugacity of the vent fluids are responsible for these enrichment factors. This also explains the large positive Eu anomaly, because Eu is mainly in the divalent state in the fluids, and thus, is more soluble than the other trivalent REE.

Mineralogy and Chemistry of Hydrothermal Mn-Fe Crusts

Black Mn-rich and ocher Fe-rich precipitates were repeatedly observed and recovered in all four diving areas, mainly along the Valu Fa Ridge but also on top

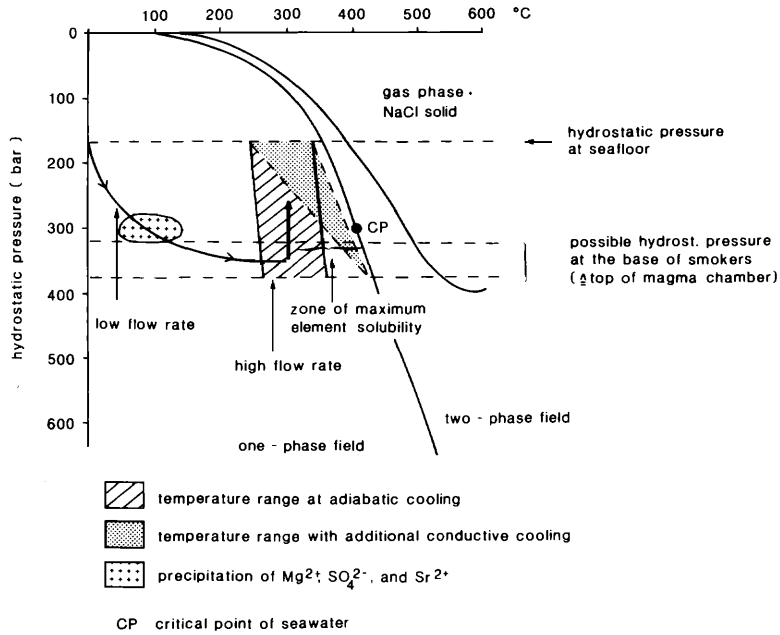

FIG. 8. P-T diagram for seawater adopted for the water depth of the Valu Fa Ridge. Possible fluid circulation pathways, drawn with data from Rosenbauer and Bischoff (1983) and Cowan and Cann (1988).

of seamounts east of the northern Valu Fa Ridge (Fig. 1) and east of the central Valu Fa Ridge. Mn-Fe precipitates coat and impregnate surface rocks and form small chimneys and up to 10 m high mounds.

The hydrothermal Mn oxide crusts of the Valu Fa Ridge are significantly enriched in Mn, Na, and Mo compared to hydrogeneous Mn crusts of off-ridge areas (von Stackelberg et al., 1990a; Table 3). They are mainly composed of well-crystallized birnessite and/or todorokite, and some manjiroite. Ocher-colored Fe-rich material, commonly found underneath Mn oxide crusts, is mostly amorphous and sometimes contains goethite and nontronite. For the nontronite from a seamount east of Valu Fa Ridge, Stoffers et al. (1990) obtained an oxygen isotope temperature of formation of 22°C. Spherical and filamentous growth structures of Mn and Fe crusts are comparable in shape and size to bacteria which may have enhanced

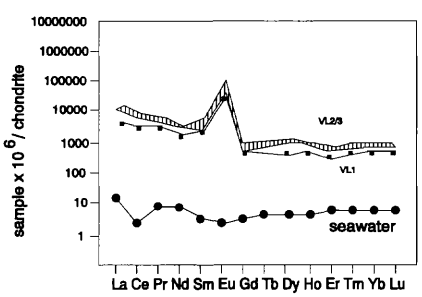

FIG. 9. REE end-member fluid concentrations normalized to chondrite vs. atomic number for the Vai Lili vent site. Seawater is shown for comparison.

TABLE 3. Representative Analyses of Mn-Fe Precipitates

Sample no. Location	NL 10 09 White Church	NL 20 05-2 Vai Lili	NL 16 07-1 Hine Hina	NL 19 05-1 Vai Lili
SiO_2 (%)	00.29	00.39	00.09	17.26
Fe_2O_3	00.25	00.22	00.29	41.19
Al_2O_3	00.13	00.05	00.13	01.48
MnO	63.86	66.06	67.33	00.75
MgO	03.14	03.33	01.11	01.42
CaO	02.48	01.95	01.87	03.95
Na_2O	03.41	02.90	06.31	02.61
K2O	00.48	01.30	00.20	00.68
P_2O_5	00.04	00.06	00.04	03.93
SO_3	00.26	01.56	00.23	00.30
L.O.I.	24.91	21.66	22.08	25.89
Total	99.25	99.48	99.68	99.46
As (ppm)	111	28	17	23
Ba	1,014	6,431	214	186
Co	7	26	9	<7
Cr	86	102	84	46
Cu	96	610	39	<10
Mo	1,615	600	644	<4
Ni	85	70	28	<7
Pb	<10	<10	10	<10
Sr	511	643	224	765
Zn	358	447	110	16

L.O.I. = loss on ignition

mineral deposition (Juniper and Fouquet, 1988; von Stackelberg et al., 1990b).

White material composed of bleached and altered volcanic rocks was found at the Hine Hina field on the southern Valu Fa Ridge (Fig. 4). The white material is composed of angular volcanic rocks of gravel to coarse sand size with different stages of alteration and mineralization. This alteration process progrades from the outer surface to the center of rock fragments. In other areas, rocks are completely altered and disintegrated to a white sand. Glittering, nonoxidized pyrite crystals at the surface of the white sand were observed on a slope and sampled with the submersible. Downslope gliding of the white sand apparently brings fresh material to the surface. The white material is predominantly amorphous and contains alunite, pyrophyllite, cristobalite, and opal-CT (Herzig et al., 1990a; von Stackelberg et al., 1990a). Sulfide mineralization forms disseminated crystals or veinlets. SEM photographs show marcasite as well as pyrite. The pyrite grains are euhedral and scattered as single crystals. The latter belong to two main grain size fractions—small crystals less than 30 μm and large crystals up to 150 μm—or the pyrite grains form round and irregular porous aggregates. Some euhedral grains are coated by a thin film of probable Ti phases (sphene and anatase?).

Additional dark fragments mainly of andesite were found with whitish-gray altered outer zones of sulfide impregnation, including pyrrhotite (either intergrown with or replaced by pyrite) and pyrite in four main textural variations (small dense grains intergrown with pyrrhotite; framboidal aggregates; massive grains developed from porous or framboidal aggregates; porous aggregates). Spherical framboidal pyrite is in part enveloped in goethite (stable association), followed by melnikovite pyrite. The massive pyrite grains are frequently intergrown with marcasite, and rarely with sphalerite or hematite. In view of the elevated temperature of the discharging water and the increased density of vent biota, the white patches indicate a higher level of hydrothermal activity than neighboring areas covered with Mn-Fe crusts. Very commonly they are separated from each other by ridge-parallel fractures. The low-temperature deposits of crusts and white zones were observed along the crest of the southern Valu Fa Ridge for a distance of about 4 km.

Mineralogy of Sulfide Deposits

The relative mineral abundance for the three main areas is presented in Figure 10. We present here major characteristics for each field and each mineralogical group. Samples are shown in Figure 11.

Hine Hina deposits (area 1)

Ba-Zn chimneys: The chimneys are mainly composed of early barite followed by Fe-poor sphalerite. Pb and As sulfides and sulfosalts are very abundant (up to 5–10% in some samples) compared to other areas. The first minor mineral to appear is tennantite, initially as numerous small (10 μm) disseminated blebs or as dendritic growths within sphalerite. The size of the inclusions increases toward microchannels where tennantite can constitutes a continuous rim. Silver is generally highly concentrated in tennantite (up to 11 wt %). Galena is the second minor mineral to appear as idiomorphic crystals growing on tennantite. Gratonite ($Pb_9As_4S_{15}$) occurs as epitaxic growths on galena. Another unidentified Pb-As sulfosalt (perhaps a fine mixture of two sulfosalts) is common, generally independent of galena and other sulfosalts, as a spherolitic rims on sphalerite around microconduits.

Fe-Cu massive sulfides (Fig. 11h): These samples were collected from sulfide outcrops beneath the manganese crust within the highly altered andesite. Barite is still present, but just as a late mineral at the outer part of the samples. The massive sulfides consist entirely of pyrite and marcasite. Chalcopyrite is enriched around decimetric channels within the mas-

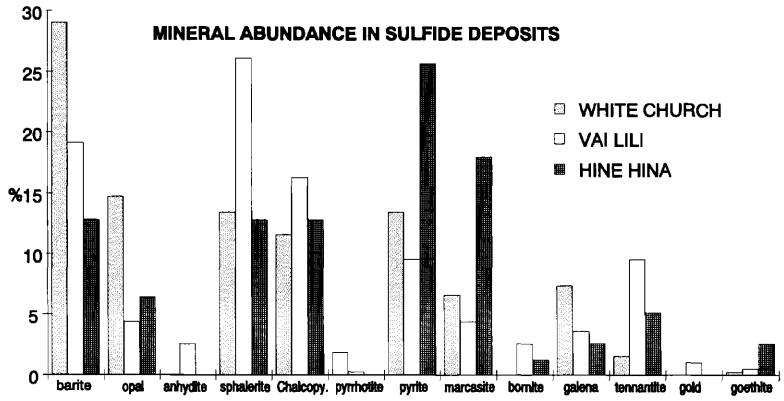

FIG. 10. Comparison of mineral abundance in the three main hydrothermal field.


a
b
1CM
c
1CM
d
e
f
g
h

sive sulfide, and locally, within coarsely layered massive sulfides cementing around andesitic gravels.

Vai Lili deposit (area 2)

In this area a complete cross section through a sulfide deposit was established. The following section describes the paragenesis for the different portions from top to bottom. The paragenetic succession for each portion is presented in Figure 12.

Ba-Cu chimneys (Fig. 11a): These display the typical mineralogical zonation of a black smoker, the main difference being the occurrence of barite instead of anhydrite at the outer part of the chimneys as is typically found on the midocean ridges. Anhydrite is present only in two samples from active chimneys. The absence of anhydrite in older samples is due to its dissolution and replacement by barite. Near the inner chalcopyrite wall, barite occurs as tabular crystals typical of crystallization under stable conditions. At the outer part of the chalcopyrite zone, dendritic crystals indicate rapid crystallization due to rapid cooling under unstable conditions. Chalcopyrite from the inner wall commonly replaces sphalerite by a chalcopyrite disease process (Barton and Bethke, 1987). In old chimneys, chalcopyrite is partly oxidized to bornite and covellite. At this level, secondary magnetite and hematite are common. Galena and marcasite occur at the outer part of the chimney associated with amorphous silica and Fe oxides. Tennantite occurs as small inclusions (a few μm) near the chalcopyrite zone. X-ray diffraction analysis indicates that wurtzite is only abundant in active chimneys.

Ba-Zn chimneys (Fig. 11c): At the outer part, dendritic barite is the first mineral to precipitate, followed by dendritic sphalerite. Galena and some Pb-As sulfosalts are the last minerals to precipitate. In samples from active white smokers, barite-sphalerite-galena was clearly the first mineralogical association to precipitate in contact with seawater. Toward the inner part, galena disappears and the crystallinity of sphalerite increases progressively, together with the crystallinity of barite. The amount of barite progressively decreases. Tennantite and chalcopyrite are seen in homogeneous sphalerite very often at the contact between the early white dendritic sphalerite and the well-crystallized darker sphalerite. Locally, tennantite is particularly abundant and associated with primary bornite. Chalcopyrite can occur as exsolutions in bornite. In places the amount of tennantite increases around microchannels. In this environment, grains of primary native gold were found in sphalerite and more rarely in tennantite (see Herzig et al., 1990, 1993). However, gold is more abundant at the core of the chimneys where the mineralogical assemblage is very simple with large crystals of sphal-

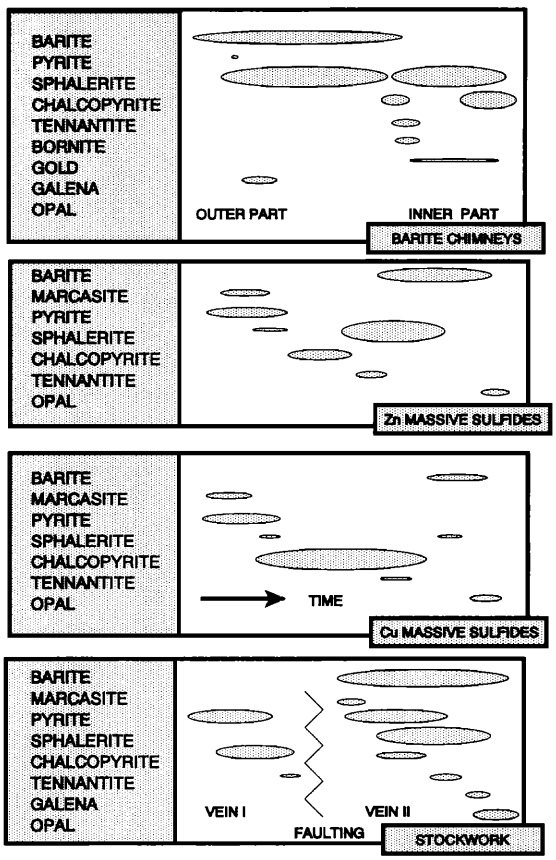

FIG. 12. Paragenetic successions at different levels across the Vai Lili sulfide deposit.

FIG. 11. a. White smoker chimney (top is at the right). Chalcopyrite forms a continuous layer (yellow) around the inner conduit. The outer part (gray) is predominantly barite, with minor sphalerite and anhydrite (Vai Lili field). b. Barite-sphalerite sample from the surface of the mound. Primary native gold was observed in this type of sample (Vai Lili field). c. Barite-sphalerite chimney. Idiomorphic crystals of barite are growing in the inner conduit (White Church field). d. Massive Zn-Cu-Fe-rich sulfides. The amount of Cu increases around a conduit in the massive sulfide (Vai Lili field). e. Massive Cu-Fe-rich sulfides (White Church field). f. Sample from the stockwork, collected on the major normal fault at the Vai Lili field; two generations of veins are seen. The first (yellow) is Cu-Fe rich, the latter is Ba-Zn rich (dark brown). g. Partly altered volcaniclastic andesite cemented by barite and sphalerite (White Church field). h. Massive pyrite and marcasite. Chalcopyrite is enriched around a central conduit. Collected in the massive layer occurring within the altered andesite at the Hine Hina field.

TABLE 4. Compositions of Sulfides from the White

A. White

	Site 1								
Sample no.	NL06 01 02	NL06 01 02-A	NL06 01 03-A	NL10 01	NL10 04a	NL10 04b	NL10 04-A	NL10 05	NL10 05-A
Type	II	II	II	II	II	II	II	II	II
SiO_2 (%)	15.82	20.4	18.4	19.56	29.89	28.05	21.8	11.20	15.1
Al_2O_3	1.08	<1	<1	1.02	1.12	1.07	<1	0.95	<1
S	15.85	12.9	15.4	15.77	18.54	18.55	17.6	16.22	14.5
Ca	0.10	0.20	0.20	0.09	0.09	0.07	0.08	0.06	0.20
Fe	3.23	1.80	3.50	3.67	5.53	6.08	5.08	2.26	3.10
Cu	0.26	0.11	0.15	0.25	0.35	0.41	0.16	0.30	0.08
Zn	6.24	2.60	4.70	6.32	14.36	12.54	8.10	6.77	0.30
Ba	37.33	42.30	39.50	34.67	19.79	21.59	33.10	41.16	46.20
Total	79.91	80.31	81.85	81.34	89.67	88.35	85.84	78.91	79.48
O	17.40	19.71	18.41	16.15	9.22	10.06	15.42	19.18	21.53
Total	97.30	100.02	101.26	97.49	98.89	98.41	101.26	98.09	101.01
Mn (ppm)	820	580	620	580	945	945	860	300	405
Co	<5	5	5	<5	<5	<5	<5	<5	<5
Ni	<20	<20	<20	<20	<20	<20	<20	<20	20
As	550	337	435	540	582	588	552	204	655
Se	<1	<1	<1	4	<1	<1	4	<1	<1
Sr	6,870	7,870	7,620	5,900	4,270	3,610	4,980	3,680	12,200
Mo	12	14	15	25	47	36	30	13	11
Ag	174	100	110	149	145	149	140	88	125
Cd	71	25	80	82	217	216	95	162	<10
In	<10	<5	<5	<10	<10	<10	<5	<10	<5
Sn	<10	<10	<10	<10	<10	<10	<10	<10	<10
Sb	155	90	93	112	133	120	100	58	65
Pb	8,500	6,380	3,840	6,150	3,760	4,270	5,170	4,320	3,420
Hb (ppb)		1,000	510	>1,000		>1,000	650		>1,000
Au (ppb)	2,880		1,600	2,900	3,500		4,000		3,000

B. Vai

Sample no.	NL20 04	NL20 04 01	NL20 01-a	NL18 05-A	NL18 05	NL20 01b	NL22 01-A	NL20 03	NL18 04-A
Type	I	I	I	II	II	II	II	II	III
SiO_2 (%)	0.29	0	3.50	1.9	1.26	0.14	<0.5	0.09	0
Al_2O_3	0.29	0	0.26	<1	0.50	0.37	<1	0.50	0.5
S	27.67	34.2	26.43	23.9	24.66	25.31	27.4	26.29	29.2
Ca	14.23	1.3	0.17	0.06	0.22	0.18	0.13	0.20	0.11
Fe	7.41	29.3	14.23	0.55	0.50	0.28	<0.5	0.25	<0.5
Cu	10.23	34	17.54	1.08	1.25	1.59	0.63	1.50	0.67
Za	13.63	0.5	15.14	34.80	37.77	39.98	45.60	48.27	47.61
Ba	7.51	0.8	16.25	27.30	24.35	23.10	16.00	15.10	14.80
Total	81.23	100.10	93.52	89.59	90.50	90.94	89.76	92.19	92.89
O	3.50	0.37	7.57	12.72	11.35	10.76	7.46	7.04	6.90
Total	84.73	100.47	101.09	102.31	101.85	101.70	97.22	99.22	99.79
Mn (ppm)	70	<50	6,500	55	<50	205	55	60	60
Co	<5	<5	<5	<5	<5	<5	<5	<5	<5
Ni	<20	<20	<20	25	20	25	28	25	25
As	170	<10	457	1,280	2,510	1,880	2,830	1,920	2,100
Se	<1	3	<1	<1	<1	<1	1	<1	<1
Sr	2,690	280	1,500	2,660	2,320	3,380	1,990	2,460	1,980
Mo	12	<2	25	35	22	10	<2	8	<2
Ag	37	22	83	170	180	243	187	173	212
Cd	385	17	543	1,270	1,268	2,032	857	1,384	1,145
In	149	305	469	70	24	100	<5	<10	<5
Sn	10	76	25	<10	<10	<10	<10	<10	<10
Sb	17	<10	90	135	123	120	<10	24	17
Pb	140	<20	780	1,010	2,200	1,650	7,590	2,630	6,220
Hg (ppb)	26		260	930		>1,000	>1,000	>1,000	>1,000
Au (ppb)	150		1,300	2,900		4,800	31	310	400

Church, Vai Lili, and Hine Hina Hydrothermal Fields
Church

Site 1			Site 2					Site 3			
NL10 06	NL10 07	NL10 07-A	NL07 06 02	NL07 07	NL07 07-A	NL07 08b	NL07 08	NL08 06	NL08 06-A	NL08 07-A	NL08 07
II	II	II	II	IV	IV	V	V	IV	IV	II	II
6.95	15.15	15.8	6.88	4.92	1.3	68.09	61.97	1.66	2.5	32.1	56.40
0.91	0.80	<1	0.42	0.71	<1	6.81	5.47	1.01	1.8	<1	1.89
14.29	12.57	14.4	34.04	31.73	35.7	6.89	8.19	33.41	33.7	14.4	10.71
0.04	0.10	0.10	0.10	0.05	0.04	0.02	0.97	0.06	0.02	0.08	0.11
0.81	0.49	1.40	14.08	30.58	32.20	3.70	7.24	11.56	6.00	2.10	3.99
0.12	0.11	0.15	0.80	29.14	30.60	0.16	0.11	9.99	5.00	0.39	1.16
2.16	0.88	5.30	36.08	0.93	0.36	0.67	0.49	45.27	54.90	11.40	12.49
49.15	44.85	43.70	3.94	0.08	0.00	7.83	4.93	0.05	0.00	27.90	5.63
74.42	74.94	80.85	96.32	98.13	100.20	94.17	89.36	103.00	103.92	88.37	92.36
22.90	20.90	20.36	1.83	0.04	0.00	3.65	2.30	0.02	0.00	13.00	2.62
97.32	95.84	101.21	98.15	98.16	100.20	97.81	91.66	103.02	103.92	101.37	94.98
170	85	200	5,140	<50	<50	<50	405	455	1,025	425	1,160
<5	<5	<5	<5	<5	<5	7	13	<5	6	<5	<5
<20	<20	<20	<20	<20	<20	<20	<20	<20	25	<20	<20
68	244	260	2,050	146	202	115	468	177	103	342	421
<1	1	4	<1	5	7	8	2	<1	4	<1	2
6,660	6,010	4,400	1,250	9	<10	1,310	966	0	<10	3,930	629
2	3	9	60	218	195	6	41	92	214	23	40
92	128	185	170	67	40	46	<10	26	22	168	162
58	12	77	1,143	59	23	<10	20	2,054	1,730	242	306
<10	<10	<5	<10	<10	22	<10	<10	<10	<5	<5	<10
<10	<10	<10	<10	<10	10	<10	<10	<10	<10	<10	<10
29	58	120	187	32	20	82	12	<10	<10	169	145
2,600	5,080	13,900	2,890	55	81	1,360	172	65	180	2,800	3,280
>1,000		>1,000	>1,000		680		>1,000		79	>1,000	
1,600	2,300		3,700		480	420			82	3,000	

Lili

NL18 04	NL18 06	NL18 0608A	NL22 04	NL22 06-A	NL22 06	NL22 03	NL21 04-A	NL21 04
III	III	III	III	IV	IV	VI	VI	VI
0.12	0.12	0	21.08	2.3	2.16	23.90	30.3	18.75
0.45	0.63	0.3	2.99	<1	0.05	2.65	7.2	6.57
29.40	29.17	30	32.80	37.1	35.15	24.85	27.5	31.94
0.09	0.10	0.09	0.07	0.00	0.05	0.97	0.07	0.03
0.04	0.03	<0.5	22.20	29.80	30.53	14.03	21.67	25.55
1.16	0.58	0.48	1.32	27.20	29.56	4.43	5.50	8.43
53.93	55.92	54.36	11.46	3.70	1.39	10.68	0.44	0.86
13.05	10.25	9.70	3.58	0.80	0.98	10.55	3.70	4.61
98.24	96.79	94.93	95.47	100.90	99.83	92.05	96.38	96.74
6.80	4.78	4.52	1.67	0.37	0.45	4.92	1.72	2.15
104.32	101.56	99.45	97.14	101.27	100.28	96.96	98.10	98.89
70	<50	<50	480	<50	<50	960	515	360
<5	<5	<5	<5	<5	<5	9	15	8
25	25	25	<20	<20	<20	<20	<20	<20
2,960	3,320	3,280	1,270	737	640	1,670	737	595
<1	<1	<1	<1	<1	<1	<1	2	<1
1,700	2,220	2,030	242	76	82	841	1,440	392
4	1	<2	102	30	33	42	88	69
294	391	420	58	35	35	59	14	25
1,556	1,088	1,100	110	120	32	196	<10	28
<10	<10	<5	<10	170	183	42	30	47
<10	<10	<10	<10	11	15	<10	10	<10
25	<10	<10	11	40	<10	36	<10	11
4,100	8,840	8,140	3,600	153	173	1,200	113	36
		>1,000	>1,000	230		>1,000	910	
2,900	12		380	440		1,800	330	

TABLE 4
C. Hine

Sample no.	NL16 06	NL16 06-A	NL16 05	NL16 03	NL16 0502-A	NL16 02-a	NL16 02-b	NL16 01
Type	II	II	IV	IV	IV	IV	IV	V
SiO_2 (%)	0.59	0.6	3.92	4.01	5.9	0.15	0.16	
Al_2O_3	0.55	0.4	1.85	3.20	2.8	0.00	0.00	
S	28.25	29.8	45.92	47.00	48.5	45.93	51.09	
Ca	0.09	0.05	0.10	0.06	0.08	0.04	0.05	
Fe	0.02	<.5	41.67	43.05	40.10	40.89	47.22	44.8
Cu	0.25	0.24	2.30	0.49	2.54	13.22	0.35	0.28
Zn	53.61	53.40	0.61	0.11	0.04	0.02	0.00	0.81
Ba	9.61	8.80	0.41	0.36	0.00	0.03	0.04	0.1
Total	92.96	93.29	96.75	98.27	99.96	100.26	98.90	
O	4.48	4.10	0.19	0.17	0.00	0.01	0.02	
Total	97.44	97.39	96.94	98.43	99.96	100.27	98.91	

Sample NL2004 corresponds to the chimney where water sample VL3 was collected at 334°C; sample NL2001a corresponds to the chimney where water sample VL2 was collected at 285°C

Types: I = Ba-Cu chimneys, II = Ba-Zn chimneys, III = Zn-Ba massive sulfides, IV = Cu-Fe massive sulfides, V = volcanic breccia, VI = stockwork; samples were grouped by mineralogical types from to the top to the root of the deposit

erite containing inclusions of chalcopyrite (up to 100 μm). Gold is observed as individual grains in the sphalerite and often at the rim or boundary to the chalcopyrite. Tiny grains of gold (<1 μm) occur in the white outer rim of the chimney. Pyrite is very scarce in the sphalerite and mostly located at the limit between the white outer millimetric rim and the darker inner zone. Pyrite appears very commonly as brecciated grains cemented by chalcopyrite. This association is typical of the deeper part of the deposit.

Massive Zn-Ba sulfides (Fig. 11b and d): This group is relatively heterogeneous and comprises Zn-rich sulfides from the outer part of inactive chimneys and samples from the upper part of the massive body. For the first group, the paragenetic sequence is similar to that of the Zn-Ba chimneys, but barite is less abundant (Table 4b, groups II and III). For the second group described as Zn massive sulfide in Figure 12, the paragenetic sequence is the same as for Cu massive sulfides, the main difference being the relative amount of sphalerite and chalcopyrite and a decrease of barite where chalcopyrite increases.

Massive Cu sulfides (Fig. 11d and e): Chalcopyrite is the dominant mineral, with some isocubanite (detectable only by X-ray diffraction). Early pyrite associated with marcasite is the second most important mineral. Pyrite is much more abundant here than at the top of the deposits and within the chimneys. Sphalerite is rare and two generations are seen. The first generation occurs as small inclusions in the pyrite and the second postdates Cu sulfides. Barite is scarce, and in contrast to samples from the top of the deposit, occurs as a late mineral. Tennantite is associated with the Cu sulfides. As observed in the stockwork, late conduits within the Cu-rich sulfides display a lower temperature paragenesis.

Stockwork (Fig. 11f): Two generations of veins are clearly seen in the samples. The first is filled with cogenetic pyrite and chalcopyrite containing minor inclusions of sphalerite and tennantite. Pyrite and chalcopyrite also occur as isolated crystals within the andesite fragments. Marcasite is very scarce as inclusions in the pyrite. Locally, sphalerite is more abundant and is partly replaced by chalcopyrite. In the second generation of veins the paragenesis is completely different. Coarse crystals of barite typical of crystallization under stable conditions are associated with early pyrite and late sphalerite. Galena occurs as large crystals within the sphalerite.

White Church deposits (area 3)

Three distinct sites with sulfides were observed in this area (Fig. 1). Two are at the top of the ridge, but the major one is on the eastern flank. Mineral abundances reported in Figure 10 include all the deposits from the area.

Site 1: In the main area (White Church deposit), the collected samples are from chimneys or from the top of the mound. The mineralogy is dominated by barite and sphalerite. Dendritic barite (barite I) with pyrite inclusions, associated with marcasite, is the first mineral to precipitate. This barite is similar to

(*Cont.*)
Hina

Sample no.	NL16 06	NL16 06-A	NL16 05	NL16 03	NL16 0502-A	NL16 02-a	NL16 02-b	NL16 01
Type	II	II	IV	IV	IV	IV	IV	V
Mn (ppm)	60	<50	50	<50	<50	<50	155	
Co	<5	6	7	20	15	<5	<5	67
Ni	20	25	<20	<20	<20	<20	<20	<50
As	14,500	9,060	280	1,250	415	880	6,020	3,700
Se	<1	<1	40	64	39	4	<1	60
Sr	3,715	2,790	910	544	1,200	2	12	<100
Mo	2	<2	47	11	40	37	3	<2
Ag	1,545	2,150	35	144	25	126	736	150
Cd	1,594	1,805	21	<10	<10	<10	<10	53
In	<10	<5	<10	<10	<5	<10	<10	
Sn	<10	<10	<10	10	<10	<10	<10	
Sb	<10	<10	<10	14	<10	24	86	28
Pb	28,700	31,400	193	210	170	206	618	
Hg (ppb)	610	>1,000		>1,000	930	380	>1,000	
Au (ppb)	53	10		690	480	3,800	10,000	670

On the basis of Ba values, O was calculated for barite; gold values are means of several analyses of one sample (see details in Herzig et al., 1993); other elements were analyzed by XRF methods by P. Cambon, IFREMER, Brest (see details on the analytical method in Fouquet et al., 1988)

the dendritic barite formed by rapid crystallization under unstable conditions at the outer part of active chimneys from the Vai Lili site. The second stage is a major sulfide episode represented by dominant sphalerite and abundant galena with minor tennantite. Chalcopyrite occurs as inclusions in sphalerite. A second generation of large barite crystals (barite II) precipitated later, indicating crystallization under stable conditions. This barite sometimes occurs as veins in barite I and in sulfides. Amorphous silica occurs as a cement after barite II.

Site 2: At the top of the ridge at a smaller site three types of mineralization were distinguished. The first type consists of barite chimneys with a paragenesis similar to that of chimneys from site 1. The second type is hydrothermally cemented volcanic breccia (Fig. 11g) which indicates important sulfide precipitation within the brecciated material. The major difference is the presence of pyrrhotite which is never observed in the surface mounds. The altered andesite is impregnated by millimetric idiomorphic pyrite or marcasite crystals. Chalcopyrite grains with epitaxial galena are common. Pyrrhotite, typically replaced by intermediate products and marcasite, occurs as fresh crystals filling the vesicles of the andesite. In the cement, idiomorphic pyrite shows epitaxic growth of galena followed by sphalerite. Barite is dominant and occurs as tabular idiomorphic crystals. The third type is massive sulfide-talus in the vicinity of the chimneys which has a paragenesis similar to that from the core of the Vai Lili deposit. Chalcopyrite is the dominant mineral with idiomorphic pyrite inclusions. Sphalerite replaces chalcopyrite and is associated with opal.

Site 3: Massive Zn-rich sulfides were collected at the top of a second volcanic ridge in the south of area 3 (Fig. 1).

General mineralogical characteristics of the sulfide deposits and their vertical zonation are consistent along the Valu Fa Ridge. The surface of the deposits is dominated by barite, sphalerite, galena, and tennantite, and locally, native gold. This contrasts strongly with midocean ridges where the surface of the deposits is commonly composed of pyrite and sphalerite. Another difference is the importance of hydrothermal precipitates occurring as cement in the brecciated andesite or as a stockwork. Pyrrhotite, which is a common mineral on midocean ridges, is only oberved as small grains in the vesicles of the brecciated volcanics. However, for a similar paragenesis, the relative abundance of minor sulfides varies from one segment of the Valu Fa Ridge to another. For example, galena is by far the most important minor mineral at White Church, whereas tennantite is dominant at Vai Lili (Fig. 10).

Chemical Composition of Sulfide Deposits

Chemical compositions of sulfides from the three main sites are reported in Table 4 A, B, and C. Based on the mineralogy, analyses are separated into six groups corresponding to the vertical zonation of the deposits.

Correlation coefficients calculated separately for the the White Church, Vai Lili, and Hine Hina fields distinguish two main groups of elements in the three areas. The first group is represented by Zn, Pb, Ba, Ag, Cd, As, and Sb and corresponds to the chimneys and the upper part of the deposits. The second, simpler group, is characterized by Cu, Fe, and Mo and corresponds to the inner part of the deposits. The absence of pyrite and Fe-poor sphalerite in chimneys and in samples from the surface of the deposits is clearly seen in the generally negative correlation between Fe-Cu and Zn-Ba. Au correlates with the group (Zn-Ba) in the two northern areas (White Church and Vai Lili) indicating enrichment at the surface of the deposit, but in the southern area Au correlates with the second group of elements (Cu-Fe) indicating enrichment in the deeper part of the deposit. Ca was seen only in active chimneys from the Vai Lili site. Co, Ni, and Se values are uniformly very low. Unusually high In concentrations up to 470 ppm were found in the core of high-temperature Cu chimneys at the Vai Lili site.

Even though the general mineralogy, geochemical zonation, and correlation for most of the elements are similar for the three main areas and contrast with midocean ridge deposits, nevertheless, there are certain geographical variations for particular elements as is seen, for example, for As and Pb in Figure 13A. Two groups of sulfides are clearly distinguished by their Pb content, lower than 1,000 ppb in the massive Cu-Fe sulfides and higher in the Ba-Zn samples. In addition to this mineralogical distinction, a southward increase in the concentration of As is clear between the White Church field in the north and the Hine Hina field in the south. Figure 13A also shows that, in the chimneys, the correlation between Pb and As is better established for the Vai Lili field. For Ba-rich mineralizations the Pb/As ratio is 18.05 at White Church and 1.68 at Vai Lili site. This difference may be explained by a different composition (degree of differentiation) of the source rocks. At Vai Lili, the Pb/As ratio measured in the fluid (0.58) is close to that of the underlying Cu-rich massive sulfides and the Cu-rich veins from the stockwork (0.27).

In order to show better the geographical variation in Pb and As, As/Zn versus Pb/Zn for the Ba-Zn group is presented in Figure 13B. Barium is two to four times more enriched in the White Church field compared to the two other fields (Table 4 A, B, and C). The Zn content is seven to nine times lower in Ba-Zn samples from the White Church field compared to that of samples from the Vai Lili field. Thus, similar Pb concentrations at Vai Lili and White Church indicate a relative enrichment of Pb at White Church. This was clearly established in the mineralogical studies, with galena being by far the more abundant minor sulfide mineral compared to tennantite in the White Church field, and tennantite being the dominant minor sulfide at Vai Lili (Fig. 10). For the Ba-Zn paragenesis, the average Pb/Zn ratios from south to north are 560 (Hine Hina), 103 (Vai Lili), and 1,430 (White Church) and the average As/Zn ratios are 220 (Hine Hina), 52 (Vai Lili), and 83 (White Church). These variations are well illustrated in Figure 13B with the result that similar deposits on individual segments have their own distinct chemical characteristics.

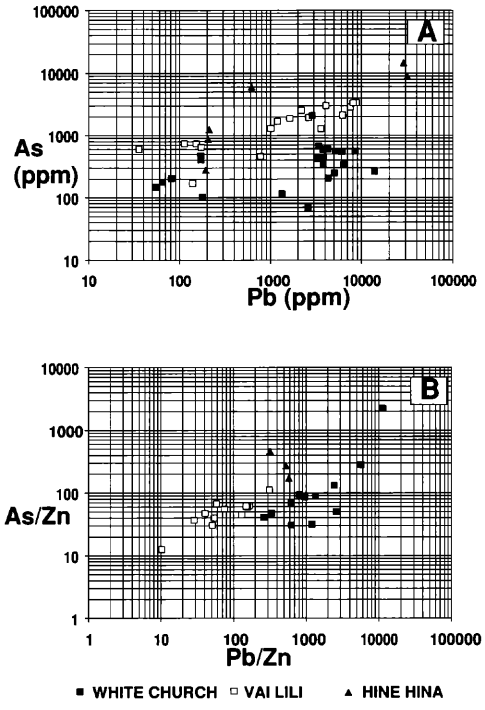

FIG. 13. a. As vs. Pb for all samples in the three hydrothermal fields. Pb contents lower than 1,000 ppm are found in Cu-Fe sulfides from the deeper part of the mound and the stockwork zone (i.e., zone 4 in Fig. 4a). Pb contents higher than 1,000 ppm are found in Ba-Zn massive sulfides and chimneys at the top of the deposits. The three hydrothermal fields are well separated. Pb-As correlation is better established in the Vai Lili field. b. As/Zn vs. Pb/Zn for Ba-Zn mineralizations in the three main areas. The three hydrothermal fields are well separated with respect to Pb/Zn.

In additon to Si, Pb, and Ba in the the Ba-Zn group, a southward decrease is seen for some other elements. Mean Au values show a clear southward decrease. This variation is spectacular for the average Au (ppb)/Zn (%) ratio which is respectively 462, 34, and 0.8 for the White Church, Vai Lili, and Hine Hina fields. The average Ag/Zn ratio does not show a systematic southward evolution, the lowest value being at the Vai Lili field.

Discussion

A tectonic-volcanic model for the formation of sulfides in back-arc environments

The Valu Fa Ridge shows a northward-increasing influence of tectonic activity as noted by von Stackel-

berg (1990) and Wiedicke and Kudrass (1990). It is thus concluded that the present-day volcanic activity is most important at the southern propagating tip of the ridge system. We now have a better understanding about the relation of hydrothermal deposits to the volcanic-tectonic activity along the ridge. The style of hydrothermal discharge, focused versus diffuse, and the morphology and type of associated hydrothermal deposits is clearly related to the style of the faulting system (Fig. 14). The three main deposits are in relatively different structural settings.

At Hine Hina (Fig. 14A) volcanic activity is prominent, the top of the ridge is made up of autobrecciated volcanic rocks and volcaniclastic sediments. The thickness of this material is not clearly established. However, observations on the flank of the ridge suggest that massive lava with open cracks exists under the volcaniclastic sediments and breccias. The estimated thickness for this brecciated material is up to 50 m. Thus, the hydrothermal system is divided into two parts. The deeper part has a focused discharge along faults in massive lava. At the volcanic stage there are no major faults in the volcaniclastic material and the upper part of discharge is diffuse and involves significant mixing with seawater (Fig. 14A). This model produces widespread low-temperature discharge and associated Mn-Fe deposits at the surface. The Fe-Mn crusts covering the area represent a first stage of hydrothermal activity (broad discharge through permeable vesicular and brecciated basaltic andesites), locally associated with small cauliflower-shaped Mn oxide mounds (more focused discharge) (Figs. 2 and 4b). The Fe-Mn oxide crusts and the hydrothermally cemented sediments (fossil ripple marks were seen) led progressively to a near-surface sealing of the hydrothermal system. This prevented any further substantial mixing with seawater and caused intensive subsurface alteration of the volcanics by circulating hydrothermal fluids of a second, higher temperature stage. These higher temperature fluids circulated horizontally below the hardened sediments, causing massive Cu-Fe sulfides to precipitate as horizontal layers beneath the crust. Locally, Ba-Zn chimneys are formed on top of the sediment. This model decribes a new type of sea-floor hydrothermal mineralization.

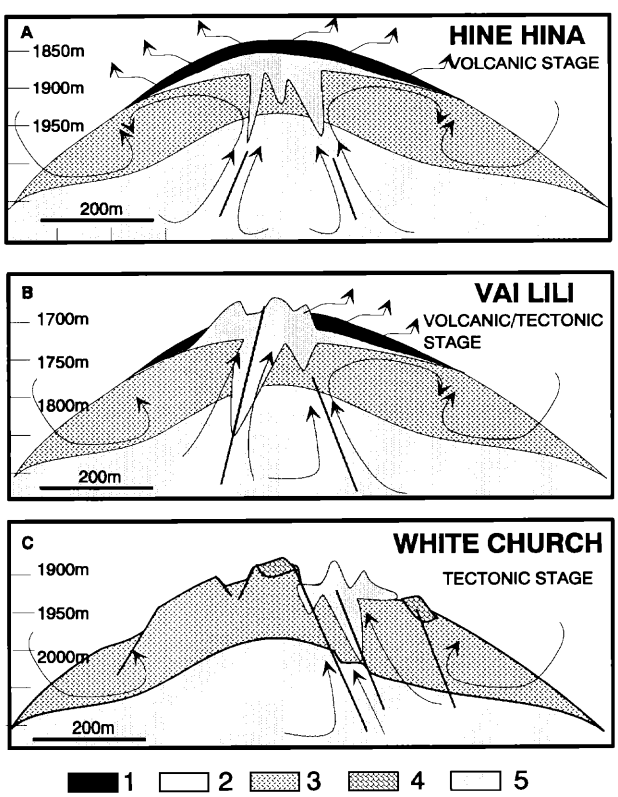

FIG. 14. Schematic vertical section across the three main hydrothermal deposits (see Fig. 2). This illustrates, from south to north, the changes in the hydrothermal discharge and morphology of deposits in relation to tectonic activity versus volcanic activity. 1 = Fe-Mn crust and sulfide impregnation in volcaniclastic material (thickness not to scale); 2 = massive sulfides; 3 = brecciated andesite; 4 = pillow lava field, 5 = massive andesite.

Vai Lili on central Valu Fa Ridge (Fig. 14B) is probably at a more evolved stage of tectonic activity. Even so, most of the ridge is made up of volcaniclastic material. Normal faults are more numerous near the top of the ridge and major faults have reached the surface through the volcaniclastic material. There is now at the surface both a focused hydrothermal discharge along a normal fault, and diffuse discharge associated with Mn Fe precipitates (Fig. 14B). Thus the sulfides are not only formed within the volcaniclastics but occur as chimneys and mineralogically zoned massive sulfide mounds on the sea floor. At the same time, a stockwork is forming along the faults (Fig. 11f). The water/rock ratio obtained for the fluid is close to that in other oceanic hydrothermal fields; this may indicate a similar plumbing system in the deeper part of the ridge. The reaction zone, estimated from quartz barometry to be at about 1 km deep, is located 2 km above the top of the seimically imaged magma chamber (Morton and Sleep, 1985; Collier and Sinha, 1990).

At White Church on northern Valu Fa Ridge (Fig. 14C), the extent of faults along the ridge was clearly established by a side-scan sonar survey (Wiedicke and Kudrass, 1990) and confirmed during the dives. Near the hydrothermal field whose location is controlled by a major fault, there is no evidence for widespread Mn-Fe deposits. The distribution of Mn chimneys is also controlled by faults indicating the importance of fault control on even low-temperature discharge. The sulfides occur as Ba-Zn chimneys and massive sulfides on the sea floor. However, the presence of hydrothermally cemented volcanic breccia indicates (Fig. 10g) that important sulfide precipita-

tion occurs within the oceanic crust and probably in stockworks rooted in the fault underneath.

There are thus, from south to north, three different morphological types of deposits. These differences can be well explained by the different tectonic styles along the ridge. The morphology of the massive sulfide deposit during the early volcanic stage (Hine Hina field) contrasts sharply with the general mound-shaped deposits on midoceanic ridges. However, in the three main areas a good case can be made that an important part of the sulfides was precipitated within the volcanic edifice as cement in the volcaniclastic rocks, as stockwork zones, or as massive sulfides.

Hot fluid chemistry

There is a long-standing debate about the role of Cl in submarine hydrothermal fluids, especially the strong chloride enrichment in some fluids (e.g., Campbell and Edmond, 1989). Cl concentrations in Vai Lili fluids are about 1.5 times higher than in ambient seawater (Table 2). The mechanisms which have been proposed to explain Cl enrichment are rock hydration, phase separation, mixing with deep brines formed by phase separation, dissolution of a retrograde soluble Cl-rich phase, and trapping of mantle-derived Cl-rich fluids (Von Damm and Bischoff, 1987; Bischoff and Rosenbauer, 1989; Campbell and Edmond, 1989).

Rock hydration can account for no more than about 5 percent of the Cl enrichment (Scott, 1987). Because Cl/Br ratios are lower than seawater, the hypothesis of the involvement of a Cl-rich mineral phase is excluded for Vai Lili fluids (see Campbell and Edmond, 1989). We do not see any evidence for exhalations of mantle-derived chlorine. From the gas concentrations measured in these fluids, recent boiling (or subcritical phase separation) can be excluded. Active phase separation below the critical point of seawater (boiling) would have resulted in a strong depletion of volatiles in the high-salinity fluids, which is not in accord with our gas data. Thus, the Cl enrichment in Vai Lili fluids can be best explained by supercritical phase separation and/or mixing with a crustal brine. From our data it is most likely that the Vai Lili fluid chemistry is mainly controlled by the interaction of seawater with andesitic basement rocks at greenschist facies conditions.

The volumes of gases extracted from Vai Lili white smokers (170–350 ml/l; Charlou et al., 1991; Erzinger and Charlou, 1991) are on the same order of magnitude as those obtained for East Pacific Rise and southern Juan de Fuca samples (Evans et al., 1988). CO_2 concentrations are close to midocean ridge systems. However, the volumes of minor gases such as CH_4 (0.07–0.11 ml/kg) and H_2 (0.57–0.77 ml/kg) are 10 to 20 times lower than those at midoceanic ridges where CH_4 is close to 2 ml/kg (1–3) and H_2 between 3 and 36 ml/kg (Evans et al., 1988).

The H_2S concentration was not directly measured, but because the total amount of analyzed gases is close to (within 5 ml) the volume of extracted gas, the H_2S content in the white smoker fluids must be relatively low and probably less than 5 ml/kg (about 1–2% of the total amount of gas). The white color of the fluid is due to the absence of H_2S, and thus, little precipitation of sulfides in the smoke. Particles from the white smoke consist primarily of barite, some anhydrite and minor sulfides. This is consistent with the absence of an H_2S smell from the Vai Lili fluid compared to midocean ridge black smoker fluids where the H_2S content ranges from 50 to 240 ml/kg (von Damm et al., 1985a and b; Bowers et al., 1988; Campbell et al., 1988a, b; von Damm, 1988; Edmond et al., 1990). Thus, the amount of H_2S, as well as that of H_2 and the CH_4, of the Vai Lili white smoker fluid is probably 10 to 20 times lower than that in midocean ridge fluids.

Even though there is no clear explanation for the very low pH of the vent fluids, some hypotheses can be discussed. In particular, conductive cooling associated with extensive Fe-Cu sulfide precipitation within the volcanic rocks may partly explain the low pH. At the three sites there are sulfide deposits within the volcanic edifice, occuring as stockwork (Vai Lili, Fig. 11f), impregnation of volcanic breccia (White Church, Fig. 11g), or as massive sulfides (Hine Hina, Fig. 11h). This, together with the observation of hydrothermally altered dacitic to andesitic xenoliths with sulfides in fresh andesite to basaltic andesite from the Vai Lili field (Herzig, et al. 1990a; von Stackelberg et al., 1990a), may indicate that an important zone of sulfide mineralization occurs beneath the hydrothermal fields. Precipitation of Cu-Fe sulfide will lower both the pH and the H_2S content of the fluid by means of reaction of the type: $Me^{+2} + H_2S \rightarrow MeS + 2H^+$.

This hypothesis was proposed to explain low pH (3) and low H_2S concentrations in the vent fluid from the TAG area at the Mid-Atlantic Ridge (Edmond et al., 1990). In the Lau basin, the predominance of brecciated rocks provides a more effective means for such widespread subsurface mineralization (von Stackelberg et al., 1988, 1990b).

The metal content in the fluid is much higher than that described for midocean ridge systems (Table 2). This is particularly so for Zn, Cd, Pb, As, and Mn. By comparison, amounts of Cu and Fe are not larger. Since Fe and Cu sulfides (pyrite and chalcopyrite) are the major components of the subsurface sulfides, their relatively low amounts in the end-member fluid and their positive correlation with temperature may be explained by widespread precipitation of Fe and Cu in the subsurface volcanic zones. This explanation is consistent with the low H_2S content and low pH of the vent fluids. A similar explanation was given to explain low Fe contents in end-member fluids at Ax-

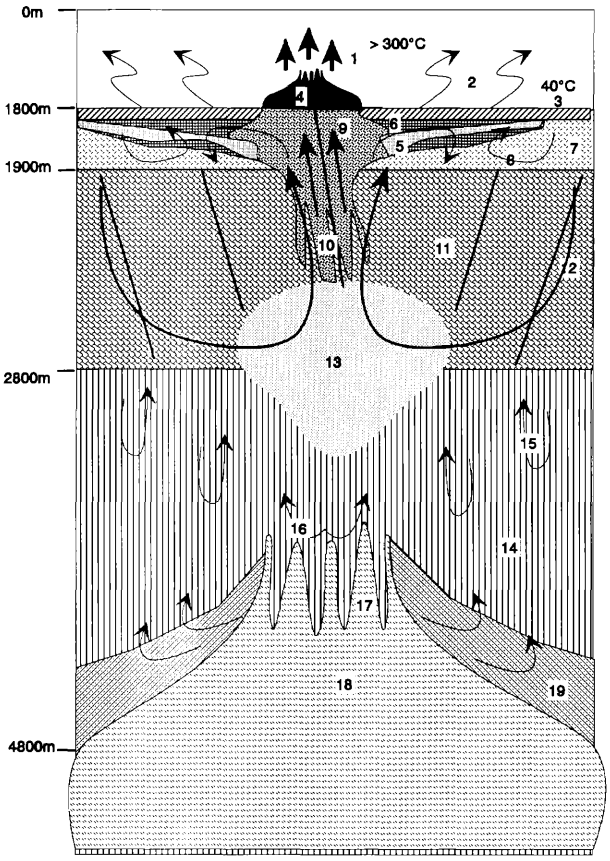

FIG. 15. Idealized vertical section under the southern Lau basin hydrothermal fields. 1 = focused high temperature discharge related to a major fault (tectonic stage); 2 = diffuse low-temperature discharge related to the volcanic stage; 3 = Fe-Mn crusts and impregnations in the volcaniclastic material; 4 = Ba-Zn mound related to the high-temperature discharge; 5 = Fe-Cu massive sulfide within the volcaniclastic material under the Fe-Mn crust; 6 = sulfide impregnation within the altered volcaniclastic material; 7 = highly porous, vesicular, and brecciated andesite; 8 = mixing between hot fluids and cold seawater within the brecciated andesite, due to the absence of faults in the volcaniclastic material during the volcanic stage; 9 = massive Cu-Fe sulfides at the base of the mound related to focused discharge along major faults during the tectonic stage—due to the temperature of the black smokers and the depth, subcritical phase separation (boiling) may be produced in this area; 10 = stockwork mineralization (Cu-Fe) possibly enhanced by fluid phase separation—the important precipitation of sulfides in the stockwork may explain the low pH and H_2S in the white smoker fluids; 11 = massive faulted andesite, open faults and fissures in this material provide pathways for water convection; 12 = recharge of cold seawater along lateral faults; 13 = reaction zone estimated to be at 1 km under the sea floor—the size and morphology of this zone is not known and its location is probably related to a change in the permeability between the fissured lava flows and the less tectonized sheeted dike complex; 14 = dike complex; 15 = deep seawater circulation restricted to the margin of the dikes—supercritical phase separation may produce brines here and contribute to an increase of the salinity in the main hydrothermal convection cells above; 16 = magmatic fluid— there is no evidence for contribution from a magmatic fluid in our samples; however due to the high H_2O content of the lava, the magmatic fluid input is probably more important here than at midocean ridges; 17 = recent dike; 18 = magma chamber located at 3 km beneath the sea floor; 19 = gabbro or more differentiated crystalline rocks.

ial Seamount (Hannington and Scott, 1988) and the Guaymas basin (Bowers et al., 1985), but at Axial Seamount subsea-floor precipitation of Fe has not affected pH, H_2S, or H_2. Low pH can also be due, in part, to interaction with highly differentiated rocks. Hajash and Chandler (1981) described experiments on the interaction between seawater and basalt, andesite, and rhyolite, showing an inverse correlation between the initial Si content of the rock and the final pH of the solution. By this model, the Si-rich rocks of the Valu Fa Ridge should result in vent fluids of low pH.

The high metal values cannot be explained by higher contents of these elements in andesites compared to MORB (Table 1). However, we note, along the Valu Fa Ridge, a positive correlation between the Si content in the volcanic rocks and Pb, Zn, and Ba, and a negative correlation between Si and Cu (Fig. 6). Thus the amount of highly differentiated rocks available for leaching may contribute to higher Pb and Zn contents in the fluid. The greatest amount of differentiated rocks is probably found in the older tectonically dominated northern segment, and deposits from this area are enriched in Pb.

The location of the reaction zone at 1 km below the sea floor possibly conforms to the boundary between tectonized volcanic flows and the dike complex. Recent studies in the Oman ophiolite have demonstrated a clear difference in the water circulation regimes in these two environments (Nehlig and Juteau, 1988). On the Valu Fa Ridge two different convective regimes can be expected, one in the upper porous and tectonized andesite as cells that are transverse in the porous andesites and longitudinal along faults. A second and deeper convective system would occur as longitudinal cells along the contact between the dikes (Fig.15). The double diffusive convection proposed by Bischoff and Rosenbauer (1989) is possible in such an environment. The deep brines could be produced by phase separation or/and input of magmatic fluid in the dike complex and within the underlying gabbro. The area of heat transfer between the two convective systems, the salinity increase of the upper cells produced by mixing with the brine, and the reaction zone (for the upper cells) may all be located at the upper zone of the dike complex (Fig. 15).

Mineralogy and geochemistry of sulfides

The vertical zonation of the deposits contrasts strongly with midocean ridge systems where the top of deposits consists of pyrite and marcasite with a variable amount of sphalerite and rare barite. Another

TABLE 5. Compositions of Sulfide Deposits from Different Oceanic Environments

		Cu	Fe	Zn	S	SiO_2	Ba	Ca	Mn	Sr	Hg	Sn	Ag	As	Sb	Pb	Co	Se	Ni	Cd	Mo	Au
				(wt %)										(ppm)								(ppb)
	1 Galapagos	4.48	32.60	4.02	32.40	21.50	0.04	0.30	542	28	5	18	46	139	11	420	288	65	16	109	129	345
	2 Snake Pit	12.42	35.47	7.00	30.88	4.16	0.00	0.60	444	229		33	111	364	32	665	228	120	21	270	71	2,180
	3 TAG	6.21	25.17	11.71	35.80	4.46	0.00	5.77	548	1,226	25	2	80	78	20	540	130	47	97	410	71	2,170
I	4 S. Explorer	3.23	25.78	4.85	28.30	7.70	7.61	1.22	865	429	11	10	122	544	38	1,100	473	100	8	161	163	777
	5 Axial Seamount	0.40	4.95	18.31	18.80	28.10	16.00	0.21	597	1,467	20	7	175	572	320	3,500	3	2	22	522	35	4,711
	6 S. Juan de Fuca	0.16	19.73	36.72	39.27	5.10	0.06	0.05	970	53	2		178	359	18	2,600	11	13	8	519	13	110
	7 EPR 13° N	7.83	25.96	8.17	35.12	5.15	0.08	4.49	100	498		<10	49	154	<10	500	968	163	<20	960	50	260
	8 EPR 11° N	1.92	22.39	28.00	35.70	1.22	0.06	0.02	775	5	2	5	38	399	30	670	16	27		886	30	154
II	9 EPR 21° N	0.58	12.44	19.76	31.41	19.00	0.15	11.21	246	1,417	2		98	296	23	2,100	14	40	3	376	22	150
	10 EPR 17°26′ S	1.25	36.25	5.55	41.00	0.20	0.00	4.70		479			31	137	9	278	270	485		148	53	100
	11 EPR 21°50′ S	2.39	28.59	21.74	40.74	3.20	0.00	0.15		14			120	110	14	515		47		665	74	364
	12 Mariana	1.15	2.39	9.96	17.80	1.20	33.33	3.71	175		22		184	126	190	74,000	2	10		465	5	784
III	13 Okinawa	1.77	7.33	22.00		16.70	2.76	0.06	1,567	1,017			2,100	27,537		142,700				950		4,600
	14 North Fiji	7.45	30.05	6.64	36.67	16.24	0.82	0.15	761	314		<10	151	182	30	571	238	168	<20	260	270	1,077
	15 Lau basin	4.56	17.40	16.10	30.12	12.45	11.56	0.56	542	1,329	>1	4	256	2,213	51	3,300	3	8	6	482	32	1,400

I = slow-spreading ridges, II = fast-spreading ridges, III = back-arc basins

Data from: 1, Hannington (1989); 2, Fouquet et al. (1993); 3, Thompson et al. (1988), Hannington (1989); 4, Hannington et al. (1990); 5, Hannington et al. (1990); 6, Bishoff et al. (1983); Zierenberg et al. (1984); 10 and 11, Fouquet unpub. data; 12, Hannington (1989); 13, Halbach et al. (1989); 14, Bendel (1993); 15, this study

difference from midoceanic ridges is the lack of pyrrhotite in the surface deposits. Pyrrhotite was observed only as the first sulfide to precipitate in vesicles of the hydrothermally cemented volcanic breccia. This implies low f_{O_2} conditions during the early stage of hydrothermal discharge. Low H_2S in the sampled fluid is not compatible with the very low Fe content in sphalerite which requires a high sulfidation state for Fe-rich fluids (Hannington and Scott, 1988). The contrasting Au parageneses between the two northern fields (Au correlated with Zn, Ag, Pb in chimneys) and the southern field (Au correlated with Fe in massive sulfides) require different geochemical processes.

The two generations of veins in the stockwork indicate a decrease in fluid temperature between two major fracturing events. This may be due to increasing porosity and mixing with seawater as brecciation along the fault increases. It indicates, during the first stage, a sudden opening of the fault, focusing discharge of nonmixed hot fluids on the sea floor. The second generation of veins with a high barite content indicates substantial mixing of ascending fluids with seawater.

In general, the mineralogy reflects the content of minor elements in the hydrothermal fluids such as Pb and As. A higher Pb content in volcanic rocks at Vai Lili is related to the higher degree of differentiation of the rocks at the surface. However, since there is no correlation between Ba and Cu with Pb in volcanic rocks and in sulfides, we have to infer either that the geochemical processes are different from one place to another or more probably that rocks from the surface are not representative of the leached rocks underneath. Even though the Ce/Pb ratio indicates a lower influence of subducted material in the Vai Lili area, the relative enrichment of Pb at White Church and Hine Hina can be better explained by a difference in the volume of highly differentiated material in the reaction zone. However, the As/Pb ratio shows a clear southward increase both in chimneys and massive sulfides. Because As was not measured in volcanic rocks, we are unable to explain this variation.

Comparison with other volcanogenic deposits

Based on comparisons between modern and ancient deposits, some theories have been expounded about the relation between the tectonic setting and composition of deposits (Scott, 1983, 1985, 1987). With new data recently obtained on modern back-arc mineralizations (Halbach et al., 1989; Fouquet et al., 1991a and b), we have now a more precise view of this relation. Compared to midocean ridge deposits (Table 5), the Lau basin mineralization is clearly distinguished by higher Ba and Zn and very low Fe contents at the surface of the deposits, higher As, Pb, Ag, Au, and Hg concentrations, and lower amounts of

Mo, Se, and Co. For numerous elements (Ba, Mo, Se, Co, Pb), the Lau basin sulfide composition is similar to that for Axial Seamount on the Juan de Fuca Ridge (Hannington and Scott, 1988), but this deposit is not representative of midocean ridge types. Compared to other back-arc basin deposits (Table 5), differences depend primarily on the maturity of the basin. In young back-arc systems formed within continental crust (i.e., Okinawa trough), As and Pb occur at much higher concentrations. In basaltic back-arc systems (e.g., North Fiji basin), the sulfide composition is close to that of midocean ridge deposits. Compared to the Mariana deposits, which are formed in a similar but basalt-controlled back-arc environment, the Lau basin deposits have higher Cu, Zn, and As but lower Ba and Pb concentrations. However, like the Lau basin, the Mariana deposits are well distinguished from midocean ridge ones by their low amounts of Se, Mo, and Co.

Although ore-forming processes in back-arc environments are similar to those described at midocean ridge spreading centers, specific properties of the fluids and deposits are largely controlled by the physico-chemical properties of the crust which in turn reflect the tectonic setting. Both mineralogical and geochemical compositions of sulfides and compositions of fluids indicate the differences between back-arc and ocean ridge environments. The vertical zonation of the Vai Lili sulfide body is close to the normal sequence of typical kuroko deposits (Ohmoto and Skinner, 1983), where the outer deposit is black ore (barite, sphalerite, pyrite, galena) and the core is yellow ore (pyrite, chalcopyrite). As in the Lau basin, the kuroko deposits are rich in Ba, Zn, Cu, Pb, and Au (Tanimura et al., 1983) and are associated with felsic calc-alkaline rocks (andesites and dacites) of a back-arc spreading center, or more precisely, a failed arc rift (Cathles et al., 1983). However, the type of deposits produced in back-arc basins largely depends on the composition of the basement rocks which, in turn, can be related to volcanic and tectonic maturity of the back-arc system (Fouquet et al., 1991a). In nascent back arcs, such as the Okinawa trough (Halbach et al., 1989), the composition of the hydrothermal system is controlled by continental crust. Partial melting of continental crust contributes to the generation of felsic magma and the resulting rocks are leached. Conversely, in mature back-arc basins, such as the North Fiji basin (Auzende, 1989) and the northern Lau basin (Hawkins and Helu, 1986; Malahoff and Falloon, 1991), the basaltic oceanic crust produces hydrothermal deposits similar to those of midoceanic ridges. Due to the presence of a differentiated series of volcanics with island-arc affinities, the Lau basin environment is considered to be intermediate between oceanic and continental back-arc settings. This intermediate position is also reflected by the mineralogical and geochemical composition of sulfide mineralization (Fig. 16). Continental crust-controlled back-arc deposits (Okinawa trough, kuroko) are enriched in Pb compared to basalt-controlled systems (North Fiji basin and midocean ridge). In the southern Lau basin, the Pb enrichment is intermediate.

The relationship of hydrothermal deposits to highly fractionated rocks can be interpreted in terms of heat supply. A large volume of differentiated rocks is related to a large magma chamber giving a maximum heat supply to drive the hydrothermal convection. In such a system, hydrothermal deposits will form at the surface, in the vicinity of the shallowest part of a magma chamber, where the thermal gradient is a maximum and where more differentiated lavas occur. This is probably now the case at the Vai Lili site, where highly differentiated rocks are associated with one of the most active hydrothermal fields in the oceans. In this area, the seismic reflector interpreted to be a magma chamber is located 3 km below the active field. This observation is in agreement with records of fossil volcanogenic deposits where it has been demonstrated that arc and back-arc environments with highly differentiated lavas are among the most favorable settings for the formation

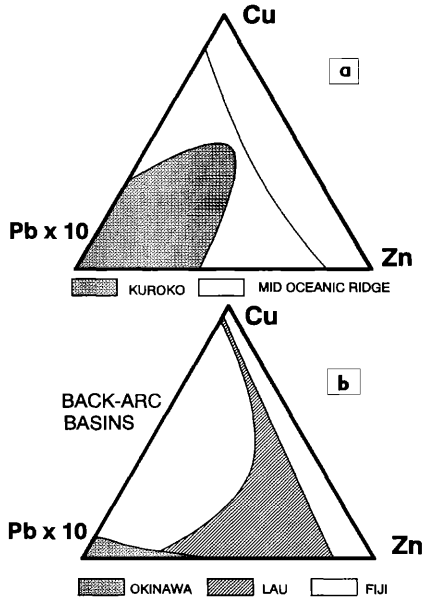

FIG. 16. Composition of submarine volcanogenic massive sulfides in different environments. a. Oceanic crust deposits versus continental crust deposits (kuroko type). b. Back-arc mineralization in relation to the maturity of the back-arc system. Deposits in young intracontinental basins (Okinawa trough) are close in composition to the kuroko type. Island-arc-controlled back-arc deposits are represented by the southern Lau basin deposits. Mature back-arc systems controlled by basaltic crust (i.e., North Fiji basin) produce deposits that have compositions close to midocean ridge mineralizations.

of large sulfide deposits (Mosier et al., 1983; Scott, 1983, 1985, 1987). In the same way, in the Noranda district in Canada, there is a strong correlation between the abundance of Archean massive sulfide deposits and felsic volcanic rocks (Franklin et al., 1981). As suggested for the Lau basin, in some ancient deposits, stockwork or stringer zones can be the most important part of the mine. For example, at the Norbec mine in Canada, the stringer sulfides were mined for 1 km below the massive ore (Franklin et al., 1981). In the Noranda area, sulfide deposits, commonly associated with submarine volcaniclastic material, are generally formed between an early felsic and a late mafic episode. The southern Lau basin is at an early stage of opening. If basaltic volcanism typical of a mature back-arc basin (i.e., northern Lau basin) is superimposed on Valu Fa, the same succession will be achieved. This is likely to happen readily in a back-arc system where the spreading centers are temporally and spatially unstable when compared to midocean ridges. Thus, there are close similarities between Precambrian deposits from the Canadian Shield and young intraoceanic back-arc deposits. There are, however, major differences in the compositions of the deposits, including the paucity of barite in Precambrian deposits and pyrrhotite in the Lau basin.

Conclusions

The Valu Fa Ridge is one of the best areas where present-day metallogenic processes in back-arc environments can be studied. The main characteristics of sulfide deposits in the southern Lau basin are presented as an idealized vertical section in Figure 15.

The morphology of the deposits is controlled by the relative interplay of volcanic and tectonic activity of the ridge segment. In the volcanic stage, early low-temperature Fe-Mn crusts are formed due to mixing between hydrothermal fluids and cold seawater within highly brecciated andesite. Sulfide deposits start to develop as stockworks, impregnations, and massive sulfides within the brecciated volcanic rocks beneath an indurated Fe-Mn crust. As the tectonic influence improves pathways, sulfidic mounds are built on the sea floor. This succession was well established from south to north along the Valu Fa Ridge.

Differences in the mineralogical and geochemical composition of the main hydrothermal fields are explained by differences in the relative amounts of leached mafic versus felsic rocks. However, variations in the contribution of subducted materials to arc volcanism does not produce a clear picture of the effect on the mineralogy and chemistry of the deposits. The vertical zonation of deposits is consistent from one deposit to another. The Fe-poor and Ba-, Zn-, As-, Pb-, and Au-rich upper part of the deposit contrasts with midocean ridge deposits.

The composition and volume of gas in the white smokers does not show any evidence for subcritical phase separation (boiling). The question is still open for black smokers where temperatures closer to the boiling point (360°C) were measured. The chlorine enrichment of the vent fluids may be explained by the mixing of convective heated seawater with deep brines produced by supercritical phase separation. Most metal concentrations in the vent fluids are much higher than those for midoceanic ridges; the relatively low Cu and Fe contents may be due to massive precipitation of sulfides within the volcanic rocks. This is compatible with field observations and can also explain the unusually low pH and H_2S content of the fluids. The estimated depth for the reaction zone (1 km) may be controlled by the boundary between the dike complex and the overlying faulted porous andesite. There is no evidence for a contribution of magmatic fluids.

Back-arc tectonic environments have a high metallogenic potential, including gold. The Valu Fa Ridge is a key to understanding the metallogenic processes that occur as maturation of a back arc increases. In nascent back-arc basins, kuroko-type mineralization influenced by continental crust is produced (e.g., Okinawa trough). During the early stage of interarc spreading, Lau basin-type deposits are produced, which have close similarities to Precambrian volcanogenic massive sulfides. In mature basins (e.g., North Fiji basin), the compositions of deposits controlled by basaltic crust are similar to midocean ridge and Cyprus types. In term of volcanic environment, tectonic setting, and chemical composition, the Lau basin deposits can be considered to be a transitional type between kuroko and midoceanic ones.

Acknowledgments

The Nautilau cruise was an IFREMER/BGR joint project to study hydrothermal activity in the Lau basin. The campaign was supported by France and Germany. We acknowledge the financial support of the Bundesministerium für Forschung und Technologie, Bonn; the Deutsche Forschungsgemeinschaft, Bonn; and the Bundesanstalt für Geowissenschaften und Rohstoffe, Hannover. We thank the crew members and the *Nautile* team, and S.L. Tongilava (Ministry of Land Survey and Natural Resources, Kingdom of Tonga) for his help and permission to work within the Tongan Exclusive Economic Zone. We are grateful to K.-P. Burgath (BGR, Hannover) for the microscopic work on the disseminated sulfide mineralization. The manuscript was improved by comments from the *Economic Geology* reviewers.

REFERENCES

Auzende, J.M., and Shipboard Scientific Party, 1989, Le cadre geologique d'un site hydrothermal actif: la Campagne STARMER 1 du submersible Nautile dans le Bassin Nord-Fid-

jien: Académie des Sciences [Paris] Comptes Rendus, v. 309, p. 1797–1795.
Barton, P.B., and Bethke, P., 1987, Chalcopyrite disease in sphalerite: Pathology and epidemiology: American Mineralogist, v. 72, p. 451–467.
Beck, F., 1990, Etude pétrologique et géochimique de la partie sud du bassin de Lau (S-W Pacifique): Unpublished Diplôme d'Etude Approfondies, Université de Strasbourg, 30 p.
Bendel, V., 1993, Cadre géologique et composition des minéralisations hydrothermales en contexte arrière-arc. Exemple de la dorsale du Bassin Nord Fijien (sud-ouest Pacifique): Unpublished Ph.D. thesis, University of Brest, 259 p.
Bendel, V., Fouquet, Y., Auzende, J.-M., Lagabrielle, Y., Grimaud, D., and Urabe, T., 1988, The White Lady hydrothermal field, North Fiji back-arc basin, southwest Pacific: ECONOMIC GEOLOGY, v. 88, p. 2237–2249.
Bertine, K., and Keene, J.B., 1975, Submarine barite-opal rocks of hydrothermal origin: Science, v. 188, p. 150–152.
Binns, R.A., and Scott, S.D., 1993, Actively forming polymetallic sulfide deposits associated with felsic volcanic rocks in the eastern Manus basin, Papua New Guinea: ECONOMIC GEOLOGY. v. 88, p. 2122–2153.
Bischoff, J.L., and Rosenbauer, R.J., 1989, Salinity variations in submarine hydrothermal systems by layered double-diffusive convection: Journal of Geology, v. 97, p. 613–623.
Bischoff, J.L., Rosenbauer, R.J., Aruscavage, P.J., Baedecker, P.A., and Crock, J.G., 1983, Seafloor massive sulfide deposits from 21° N, East Pacific Rise, Juan de Fuca Ridge, and Galapagos rift: Bulk chemical composition and economic implication: ECONOMIC GEOLOGY, v. 78, p. 1711–1720.
Boespflug, X., Dosso, L., Bougault, H., and Joron, J.L., 1990, Trace element and isotopic (Sr, Nd) geochemistry of volcanic rocks from the Lau basin: Geologisches Jahrbuch, v. 92, p. 503–516.
Both, R., and Shipboard Scientific Party, 1986, Hydrothermal chimneys and associated fauna in the Manus back-arc basin, Papua New Guinea: EOS, American Geophysical Union Transactions, v. 67, p. 489–490.
Bowers, T.S., von Damm, K.L., and Edmond, J.M., 1985, Chemical evolution of ridge-crest hot springs: Geochimica et Cosmochimica Acta, v. 49, p. 2239–2252.
Bowers, T.S., Campbell, A.C., Measures, C.I., Spivack, A.J., Khadem, and Edmond, J.M., 1988, Chemical controls on the composition of vent fluids at 13°11′ N and 21° N, East Pacific Rise: Journal of Geophysical Research, v. 93, p. 4522–4536.
Bruland, K.W., 1983, Trace elements in sea-water: Chemical Oceanography, v. 8, p. 157–220.
Campbell, A.C., and Edmond, J.M., 1989, Halide systematics of submarine hydrothermal vents: Nature, v. 342, p. 68–170.
Campbell, A.C., Bowers, T.S., and Edmond, J.M., 1988a, A time-series of vent fluid compositions from 21°N, EPR (1979, 1981, 1985) and the Guaymas basin, Gulf of California (1982, 1985): Journal of Geophysical Research, v. 93, p. 4537–4549.
Campbell, A.C., Palmer, M.R., Klinkhammer, G.P., Bowers, T.S., Edmond, J.M., Lawrence, J.R., Casey, J.F., Thompson, G., Humphris, S., Rona, P., and Karson, J.A., 1988b, Chemistry of hot springs on the Mid-Atlantic Ridge: Nature, v. 335, p. 514–519.
Cathles, L.M., Guber, A.L., Lenagh, T.C., and Dudas, F.O., 1983, Kuroko-type massive sulfide of Japan: Product of an aborted island-arc rift: ECONOMIC GEOLOGY MONOGRAPH 5, p. 96–114.
Charlou, J.L., Donval, J.P., Fouquet, Y., and Erzinger, J., 1991, Hydrothermal activity in the Lau basin: Plumes and hot fluid chemistry [abs.]: Terra Cognita, v. 3, p. 311.
Cherkis, N.Z., 1980, Aeromagnetic implications and sea-floor spreading history in the Lau basin and northern Fiji basin: Committee for Coordination of Joint Prospecting for Mineral Resources-South Pacific Offshore Areas Technical Bulletin, v. 3, p. 37–46.
Collier, J., and Sinha, M., 1990, Seismic images of a magma chamber beneath the Lau basin back-arc spreading centre: Nature, v. 346, p. 646–648.
Cowan, J., and Cann, J., 1988, Supercritical two-phase separation of hydrothermal fluids in the Troodos ophiolite: Nature, v. 333, p. 259–261.
Craig, H., Horibe, Y., Farley, K.A., Welhan, J.A., Kim, K.R., and Hey, R.N., 1987, Hydrothermal vents in the Mariana trough: Results of the first Alvin dives: EOS, American Geophysical Union Transactions, v. 68, p. 1531.
Edmond, J.M., Campbell, A.C., Palmer, M.R., and German, C.R., 1990, Geochemistry of hydrothermal fluids from the Mid-Atlantic Ridge; TAG and MARK [abs.]: EOS, American Geophysical Union Transactions, v. 71, p. 1650–1651.
Erzinger, J., and Charlou, J.L., 1991, Chemistry of hydrothermal fluids from Valu Fa Ridge, Lau basin [abs.]: Terra Cognita, v. 3, p. 52.
Evans, W.C., White, L.D., and Rapp, J.B., 1988, Geochemistry of some gases in hydrothermal fluids from the southern Juan de Fuca Ridge: Journal of Geophysical Research, v. 93, p. 15305–15313.
Foucher, J.P., and Shipboard Scientific Party, 1988, La ride de Valu Fa dans le bassin de Lau méridional (sud-ouest Pacifique): Académie des Sciences [Paris] Comptes Rendus, v. 307, p. 609–616.
Fouquet, Y., Auclair, G., Cambon, P., and Etoubleau, J., 1988, Geological setting and mineralogical and geochemical investigations on sulfides deposits near 13° N on the East Pacific Rise: Marine Geology, v. 84, p. 145–178.
Fouquet, Y., von Stackelberg, U., and Shipboard Scientific Party, 1990, Hydrothermal activity in the Lau basin, first results from the Nautilau cruise: EOS, American Geophysical Union Transactions, v. 71, p. 678–679.
Fouquet, Y., von Stackelberg, U., Charlou, J.L., Donval, J.P., Erzinger, J., Foucher, J.P., Herzig, P., Mühe, R., Soakai, S., Wiedicke, M., and Whitechurch, H., 1991a, Hydrothermal activity and metallogenesis in the Lau back-arc basin: Nature, v. 349, p. 778–781.
Fouquet, Y., von Stackelberg, U., Charlou, J.L., Donval, J.P., Erzinger, J., Foucher, J.P., Harmegnies, F., Herzig, P., Mühe, R., Pelle, H., Soakai, S., Wiedicke, M., and Whitechurch, H., 1991b, Hydrothermal activity in the Lau back-arc basin. Sulfides and water chemistry: Geology, v. 19, p. 303–306.
Fouquet, Y., Wafik, A., Cambon, P., Mevel, C., Meyer, G., and Gente, P., 1993, Tectonic setting, mineralogical and geochemical zonation in the Snake Pit sulfide deposit (Mid-Atlantic Ridge at 23° N): ECONOMIC GEOLOGY, v. 88, p. 2018–2036.
Franklin, J.M., Lydon, J.W., and Sangster, D.F., 1981, Volcanic associated massive sulfide deposits: ECONOMIC GEOLOGY 75TH ANNIVERSARY VOLUME, p. 485-627.
Frenzel, J.M., Mühe, R., and Stoffers, P., 1990, Petrology of the volcanic rocks from the Lau basin, southwest Pacific: Geologisches Jahrbuch, v. 92, p. 395–479.
Hajash, A., and Chandler, G.W., 1981, An experimental investigation of high temperature interactions between seawater and rhyolite, andesite, basalt and peridotite: Contributions to Mineralogy and Petrology, v. 78, p. 240–254.
Halbach, P., Nakamura, K., Washner, M., Lange, J., Sakai, H., Käselitz, L., Hansen, R.D., Yamano, M., Post, J., Prause, B., Seifert, R., Michaelis, W., Teichmann, F., Kinoshita, M., Märten, A., Ishibashi, J., Cserwinski, S., and Blum, N., 1989, Probable modern analogue of kuroko-type massive sulphide deposits in the Okinawa trough back-arc basin: Nature, v. 338, p. 496–499.
Hannington, M.D., 1989, The geochemistry of gold in modern sea-floor hydrothermal systems and implication for gold mineralization in ancient volcanogenic massive sulfides: Unpublished Ph.D. thesis, University of Toronto, 544 p.
Hannington, M.D., and Scott, S.D., 1988, Mineralogy and geochemistry of a hydrothermal silica-sulfide-sulfate spire in the caldera of Axial Seamount, Juan de Fuca Ridge: Canadian Mineralogist, v. 26, p. 603–625.

Hannington, M.D., Herzig, P.M., and Scott, S.D., 1990, Auriferous hydrothermal precipitates on the modern seafloor, *in* Foster, R.P., ed., Gold metallogeny and exploration: Glasgow, Blackie and Son, p. 249–282.

Hawkins, J., and Helu, S., 1986, Polymetallic sulfide deposit from a "black smoker" chimney: Lau basin: EOS, American Geophysical Union Transactions, v. 67, p. 378.

Hawkins, J.W., and Melchior, J.T., 1985, Petrology of Mariana trough and Lau basin basalts: Journal of Geophysical Research, v. 90, p. 11431–11468.

Herzig, P., von Stackelberg, U., and Petersen, S., 1990a, Hydrothermal mineralization from the Valu Fa Ridge, Lau back arc basin (SW Pacific): Marine Mining, v. 9, p. 271–301.

Herzig, P.M., Fouquet, Y., Hannington, M.D., and von Stackelberg, U., 1990b, Visible gold in primary polymetallic sulfides from the Lau back-arc: EOS, American Geophysical Union Transactions, v. 71, p. 1680.

Herzig, P.M., Hannington, M.D., Fouquet, Y., von Stackelberg, U., and Petersen, S., 1993, Gold in sea-floor polymetallic sulfides from the Lau back arc and implication for the geochemistry of gold in sea-floor hydrothermal systems of the southwest Pacific: ECONOMIC GEOLOGY, v. 88, p. 2182–2209.

Hoffman, A.W., 1988, Chemical differentiation of the earth: The relationship between continental crust and oceanic crust: Earth and Planetary Science Letters, v. 90, p. 297–314.

Jenner, G.A., Cawood, P.A., Rautenschlein, M., and White, W.M., 1987, Composition of back-arc volcanics, Valu Fa Ridge, Lau basin: Evidence for a slab-derived component in their mantle source: Journal of Volcanology and Geothermal Resarch, v. 32, p. 209–222.

Juniper, K., and Fouquet, Y., 1988, Filamentous iron-silica deposits from modern and ancient hydrothermal sites: Canadian Mineralogist, v. 26, p. 859–869.

Karig, D.E., 1971, Origin and development of marginal basins in the western Pacific: Journal of Geophysical Research, v. 75, p. 239–354.

Loock, G., McDonough, W.F., Goldstein, S.L., and Hofmann, A.W., 1990, Isotopic composition of volcanic glasses from the Lau basin: Marine Mining, v. 9, p. 235–245.

Macdonald, K.C., Fox, P.J., Perram, L.J., Eisen, M.F., Haymon, R.M., Miller, S.P., Carbotte, S.M., Cormier, M.H., and Shor, A.N, 1988, A new view of the mid-ocean ridge from the behaviour of ridge-axis discontinuities: Nature, v. 335, p. 217–225.

Malahoff, A., and Falloon, T., 1991, Preliminary report of the Akademik Mstislav Keldysh/Mir cruise 1990. Lau basin leg. (May 7–21): Suva, South Pacific Applied Geoscience Commission, unpublished cruise report 137, 12p.

Malahoff, A., Feden, R.H., and Fleming, H.S., 1982, Magnetic anomalies and tectonic fabric of marginal basins north of New Zealand: Journal of Geophysical Research, v. 87, p. 4109–4125.

McConachy, T.F., 1988, Hydrothermal plumes and related deposits over spreading ridges in the northeast Pacific Ocean: The East Pacific Rise near 11° N and 21° N, Explorer Ridge and the Tuzo Wilson Seamounts: Unpublished Ph.D. thesis, University of Toronto, 402 p.

Michard, A., 1989, Rare earth element systematics in hydrothermal fluids: Geochimica et Cosmochimica Acta, v. 53, p. 745–750.

Michard, G., Albarede, F., Michard, A., Minster, J.F., Charlou, J.L., and Tan, N., 1984, Chemistry of solutions from the 13° N East Pacific Rise hydrothermal site: Earth and Planetary Science Letters, v. 67, p. 297–307.

Morton, J., and Pohl, W., 1990, Magnetic anomaly identification in the Lau basin and North Fiji basin, southwest Pacific Ocean: Geologisches Jahrbuch, v. 92, p. 93–108.

Morton, J., and Sleep, N.H., 1985; Seismic reflections from a Lau basin magma chamber: Earth Science Series, Circum-Pacific Council for Energy and Mineral Resources, v. 2, p. 441–453.

Mosier, D.L., Singer, D.A., and Salem, B.B., 1983, Geologic and grade-tonnage information on volcanic-hosted copper-zinc-lead massive sulfide deposits: U.S. Geological Survey Open-File Report, p. 83–89.

Mühe, R., 1991, Transect along the Valu Fa Ridge, Lau basin, SW Pacific: Geochemistry of lavas from 21°50′ S–22°50′ S [abs.]: Terra Cognita, v. 3, p. 45.

Nehlig, P., and Juteau, T., 1988, Deep crustal seawater penetration and circulation at ocean ridges: Evidence from the Oman ophiolite: Marine Geology, v. 84, p. 209–228.

Ocean Drilling Program Leg 135 Scientific Party, 1992, Introduction, background, and principal results of leg 135, Lau basin: Ocean Drilling Program Proceedings, Initial Reports, v. 135, p. 5–82.

Ohmoto, H., and Skinner, B.J., 1983, The kuroko and related volcanogenic massive sulfide deposits: Introduction and summary of new findings: ECONOMIC GEOLOGY MONOGRAPH 5, p. 1–8.

Palmer, M.R., and Edmond, J.M., 1989a, Cs/Rb ratio of submarine hydrothermal fluids: Implications for nature of hydrothermal circulation: International Geological Congress, 28th, Washington, D.C., 1989, v. 2, p. 567.

—— 1989b, The strontium isotope budget of the modern ocean: Earth and Planetary Science Letters, v. 92, p. 11–26.

Parson, L.M., Pearce, J.A., Murton, B.J., and Hodkinson, R.A., 1990, Role of ridge jumps and ridge propagation in the tectonic evolution of the Lau back-arc basin, southwest Pacific: Geology, v. 18, p. 470–473.

Pelletier, B., and Louat, R., 1989, Mouvements relatifs des plaques dans le Sud-Ouest Pacifique: Académie des Sciences [Paris] Comptes Rendus, v. 308, p. 123–130.

Piepgras, D.J., and Wasserburg, G.J., 1985, Strontium and neodymium isotopes in hot springs on the East Pacific Rise and Guaymas basin: Earth and Planetary Science Letters, v. 72, p. 341–356.

Rona, P.A., 1988, Hydrothermal mineralization at oceanic ridges: Canadian Mineralogist, v. 26, p. 431–465.

Rosenbauer, R.J., and Bischoff, J.L., 1983, Uptake and transport of heavy metals by heated seawater: A summary of the experimental results, *in* Rona, P.A., Bostrom, K., Laubier, L., and Smith, K.L., eds., Hydrothermal processes at sea-floor spreading centers: NATO Conference Series, IV Marine Sciences 12, p. 177–197.

Sawkins, F.J., 1990, Metal deposits in relation to plate tectonics: Berlin, Springer-Verlag, 461 p.

Scott, S.D., 1983, Seafloor polymetallic sulfide deposits: Ancient and modern: Oceans '83, Proceedings, v. 2, p. 818–824.

—— 1985, Sea-floor polymetallic sulfide deposits: Modern and ancient: Marine Mining, v. 5, p. 191–212.

—— 1987, Sea-floor polymetallic sulfides: Scientific curiosities or mines of the future?: NATO ASI, Series C, v. 194, p. 277–300.

Stoffers, P., Singer, A., McMurtry, G., Arguit, A., and Yeh, H.-W., 1990, Geochemistry of a hydrothermal nontronite deposit from the Lau basin, southwest Pacific: Geologisches Jahrbuch, v. 92, p. 615–620.

Sunkel, G., 1990, Origin of petrological and geochemical variations of Lau basin lavas (SW Pacific): Marine Mining, v. 9, p. 205–234.

Tanimura, S., Date, J., Takahashi, T., and Ohmoto, H., 1983, Geologic setting of the kuroko deposits, Japan: Part II, Stratigraphy and structure of the Hokuroku district: ECONOMIC GEOLOGY MONOGRAPH 5, p. 9–54.

Thompson, G., Humphris, S.E., Schroeder, B., Sulanowska, M., and Rona, P.A., 1988, Hydrothermal mineralization on the Mid-Atlantic Ridge: Canadian Mineralogist, v. 26, p. 697–711.

Tufar, W., 1989, Modern hydrothermal activity, formation of complex massive sulfide deposits and associated vent communities in the Manus back-arc basin (Bismarck Sea, Papua New Guinea): Österreichische Geologische Gesellschaft Mitteilungen, v. 82, p. 183–210.

Urabe, T., and Kusakabe, M., 1990, Barite silica chimneys from the Sumisu rift, Izu-Bonin arc: Possible analog to hematitic chert

associated with kuroko deposits: Earth and Planetary Science Letters, v. 100, p. 283–290.

Volpe, A.M., Macdougall, J.D., and Hawkins, J.W., 1988, Lau Basin basalts (LBB): Trace element and Sr-Nd isotope evidence for heterogeneity in back-arc basin mantle: Earth and Planetary Science Letters, v. 90, p. 174–176.

von Damm, K.L., 1988, Systematics of and postulated controls on submarine hydrothermal solution chemistry: Journal of Geophysical Research, v. 92, p. 11334–11346.

von Damm, K.L., and Bishoff, J.L., 1987, Chemistry of hydrothermal solutions from the southern Juan de Fuca Ridge: Journal of Geophysical Research, v. 92, p. 334–346.

von Damm, K.L., Edmond, J.M., Grant, B., Measures, C.I., Walden, B., and Weiss, R.F., 1985a, Chemistry of submarine hydrothermal solutions at 21° N, East Pacific Rise: Geochimica et Cosmochimica Acta, v. 49, p. 2197–2220.

von Damm, K.L., Edmond, J.M., Measures, C.I., and Grant, B., 1985b, Chemistry of submarine hydrothermal solutions at Guaymas basin, Gulf of California: Geochimica et Cosmochimica Acta, v. 49, p. 2221–2237.

von Stackelberg, U., 1990, R.V. Sonne cruise SO48: Summary of results testing a model of mineralization: Marine Mining, v. 9–2, p. 135–144.

von Stackelberg, U., and von Rad, U., 1990, Geological evolution and hydrothermal activity in the Lau and North Fiji basins (SONNE cruise SO-35)—synthesis: Geologisches Jahrbuch, v. 92, p. 629–660.

von Stackelberg, U., and Wiedicke, M., 1990, Interpretation of bottom photographs from active spreading ridges in the Lau basin: Marine Mining, v. 9, p. 247–270.

von Stackelberg, U., and Shipboard Scientific Party, 1985, Hydrothermal sulfide deposits in back-arc spreading centers in the southwest Pacific: Bundesanstalt für Geowissenschaften und Rohstoffe, Circular 2, p. 3–14.

von Stackelberg, U., and Shipboard Party, 1988, Active hydrothermalism in the Lau back-arc basin (SW-Pacific): First results from the SONNE 48 cruise (1987): Marine Mining, v. 7, p. 431–442.

von Stackelberg, U., Marchig, V., Müller, P., and Weiser, T., 1990a, Hydrothermal mineralization in the Lau and North Fiji basins: Geologisches Jahrbuch, v. 92, v. 547–613.

von Stackelberg, U., Brett, R., and Shipboard Scientific Party, 1990b, Extended hydrothermal activity in the Lau basin (southwest Pacific): First results of R.V. Sonne cruise: EOS, American Geophysical Union Transactions v. 71, p. 1680.

Wiedicke, M., and Kudrass, H.R., 1990, Morphology and tectonic development of the Valu Fa Ridge, Lau basin (southwest Pacific): Results from a deep-towed side-scan sonar survey: Marine Mining, v. 9, p. 145–156.

Wilson, M., 1989, Igneous petrogenesis. A global tectonic approach: London, Hyman, 466 p.

Zierenberg, R.A., Shanks, W.C., and Bischoff, J.L., 1984, Massive sulfide deposits at 21° N, East Pacific Rise: Chemical composition, stable isotopes, and phase equilibria: Geological Society of America Bulletin, v. 95, p. 922–929.